ABLATION EFFICIENCY AND THERMAL DAMAGE OF INFRARED LASERS ON ex vivo LAMB BRAIN TISSUES

by

BATURAY ÖZGÜRÜN

B.Sc., in Electronics Engineering, Uludağ University, 2012

Submitted to the Institute of Biomedical Engineering
in partial fulfillment of the requirements
for the degree of
Master of Science
in
Biomedical Engineering

Boğaziçi University
2015

ABLATION EFFICIENCY AND THERMAL DAMAGE OF INFRARED LASERS ON ex vivo LAMB BRAIN TISSUES

APPROVED BY:

Prof. Dr. Murat Gülsoy (Thesis Advisor)	.....
Prof. Dr. Mehmed Özkan	.....
Assist. Prof. Dr. Özgür Tabakoğlu	.....

DATE OF APPROVAL: 18 August 2015

ACKNOWLEDGMENTS

I would like to offer my sincerest gratitude to my thesis supervisor Prof. Dr. Murat Gülsoy for his friendly guidance and contributions during my thesis.

I would like to thank to the members of my committee, Prof Dr. Mehmed Özkan and Assist. Prof. Dr. Özgür Tabakoğlu for allocating their time for critical reviewing of this thesis.

I would like to thank to Ayşe Sena Sarp, Burcu Tunç and Özgür Kaya for their friendship and partnership in the biophotonics laboratory of Boğaziçi University.

ABSTRACT

ABLATION EFFICIENCY AND THERMAL DAMAGE OF INFRARED LASERS ON ex vivo LAMB BRAIN TISSUES

The objective of this investigation is to guide to select the most sufficient infrared laser for the neurosurgery. For this reason, 1940-nm thulium fiber laser, 1470-nm diode laser, 1070-nm ytterbium fiber laser and 980-nm diode laser were operated with the ex vivo lamb brain tissues. Combination of some parameters such as brain tissue (subcortical and cortical tissues), laser output power, energy density, mode of operation (continuous and pulsed-modulated modes) and exposure time were applied.

Pre-dosimetry study was conducted to determine coagulation and carbonization onset times for the lamb brain tissues. In this way, safe operation zone could be described for the dosimetry study. In the dosimetry study, both tissues were exposed to some energy densities (2J-4J) and power levels which are 200mW-400mW-600mW-800 mW and 0.5W-1W-1.5W-2W for 1940-nm and 1470-nm laser applications, respectively. The last two laser emitted light to both brain tissues with some power levels (1W-2W-3W-4W) and energy densities (20J-40J). After each laser application, coagulation and ablation diameters were calculated under a light microscope. It was aimed to find suitable laser parameter so as to perform the greatest ablation efficiency which is determined as ablation diameter over coagulated diameter.

Consequently, 1940-nm and 1470-nm lasers created ablated and coagulated areas while the other two lasers made only coagulated areas. Ablation efficiencies were calculated for 1940-nm and 1470-nm lasers. It was found that the former and the latter can be used as a subcortical and cortical tissue ablator, respectively.

Keywords: Ablation efficiency, thermal damage, infrared lasers, lamb brain tissue, ablation, coagulation.

ÖZET

KIZILÖTESİ LAZERLERİN KUZU BEYİN DOKUSU ÜZERİNDEKİ ABLASYON VERİMLİLİĞİ VE ISIL HASARI

Bu çalışmanın amacı beyin cerrahisi için kullanılacak olan lazerin seçimine katkıda bulunmaktır. Bu nedenle, ex vivo kuzu beyini üzerinde 1940-nm tulyum fiber lazeri, 1470-nm diyot lazeri, 1070-nm ytterbium fiber lazeri ve 980-nm diyot lazeri kullanılarak deney yapılmıştır. Deneyde, bazı değişkenlerin kombinasyonu uygulanmıştır. Bu değişkenler; beyin dokusu (kortikal ve korteks altı), lazer gücü, enerji yoğunluğu, lazer çalışma yöntemi (sürekli ve module edilmiş darbeli yöntem) ve uygulama süresidir.

Ön doz çalışması, kuzu beyinindeki koagülasyon ve karbonizasyon başlama zamanlarını bulmak için yürütülür. Böylece, doz çalışması için lazerin doz uygulama aralığı tespit edilir. Doz çalışmasında, her iki beyin dokusu kullanılmış ve 1940-nm ile 1470-nm lazerler için sırasıyla 200mW-400mW-600mW-800 mW ve 0.5W-1W-1.5W-2W güç aralıkları; 2 J ile 4 J enerji yoğunlukları için uygulanmıştır. Diğer iki lazer 1W-2W-3W-4W güç aralıkları; 20 J ile 40 J enerji yoğunlukları için kullanılmıştır. Her bir uygulamadan sonra, beyin dokularında oluşan koagülasyon ve ablasyon çapları mikroskop yardımıyla ölçülmüştür. Böylece, en yüksek ablasyon verimliliği bulunarak beyin ablasyonu için uygun lazer değişkenleri bulunmak istenmiştir. Ablasyon verimliliği, ablasyon çapının koagülasyon çapına oranıyla hesap edilir.

Sonuç olarak, ablasyon ve koagülasyon lezyonları 1940-nm ve 1470-nm lazerler ile oluşturulurken diğer iki lazer sadece koagülasyon lezyonu oluşturur. Ablasyon verimliği 1940-nm ve 1470-nm lazer uygulamaları için hesaplanmış ve ilki korteks altı ablasyon işleminde başarılı olurken; ikincisi kortikal ablasyonu için uygun olduğu görülmüştür.

Anahtar Sözcükler: Ablasyon verimliliği, ısıl hasar, kızılötesi lazerler, kuzu beyin dokusu, ablasyon, koagülasyon.

TABLE OF CONTENTS

LIST OF FIGURES

LIST OF TABLES

LIST OF SYMBOLS

cm	centimeter
cm^2	square centimeter
J	Joule
mm	millimeter
mW	milliWatt
nm	nanometer
W/cm^2	Watt per square centimeter
W	Watt
g	gram
sec	seconds
μ_a	Absorption coefficient
μm	micrometer
λ	Wavelength
°C	degree Celcius

LIST OF ABBREVIATIONS

AD	Ablation Diameter
AE	Ablation Efficiency
CD	Coagulation Diameter
cm	continuous mode
CNS	Central Nervous System
CO_2	Carbon Dioxide
EM	Electromagnetic
Er:YAG	Erbium-doped Yttrium Aluminum Garnet
He−Ne	Helium-Neon
Ho:YAG	Holmium-doped Yttrium Aluminum Garnet
IR	Infrared
KrF	Krypton Fluoride
KTP	Kalium Titanyl Phosphate
LASER	Light Amplification by Stimulated Emission of Radiation
MIS	Minimally Invasive Surgery
Nd:YAG	Neodymium-doped Yttrium Aluminum Garnet
Nd:YLF	Neodymium-doped Yttrium Lithium Fluoride
PC	Personal Computer
PDT	Photodynamic Therapy
pmm	pulsed modulated mode
Tm:YAP	Thulium-doped Yttrium Aluminum Perovskite
Tm:fiber	Thulium fiber
UV	Ultraviolet
XeCl	Xenon Monochloride
XeF	Xenon Fluoride

1. INTRODUCTION

At the present time, lasers are widely used in many medical fields such as ophthalmology, dentistry and dermatology. In the history of medicine, the first medical application with a laser was operated in 1962 by Goldman. After one year, in 1963, Ruby-Laser application for cardiovascular surgery was reported by McGuff. Neurosurgeons have been interested in lasers as a ablator since 1970s because lasers could be potential tumor ablators, and some lasers provide pure spherical lesions without any carbonization which is an undesired effect and should always be avoided [1]. Conventional neurosurgical techniques take place commonly but they have some negative effects on the patients′ healthy. Physicians cannot ablate brain tumors if tumors are found inside of the brain, but they can easily remove tumors from the surface of the brain by using conventional surgical instruments and diagnostic images. However, after the surgery, some pieces of the tumor may remain that affects the overall prognosis of the treatment [2]. Physicians have to identify the blurry boundary between tumors and healthy tissue during surgery, but generally they are not be successful. Moreover, brain tumors are crucial issue in the medicine. For example, malignant gliomas which are the most common type of primary brain tumors account for just 2 percent of all adult cancer, and they cause a huge burden in long-term of disability and death [3]. Therefore, in order to perform a complete and harmless tumor resection, accurate intra-operative tumor detection system must be found. Probably, robot controlled laser system could be overcome this issue; however, primarily most efficient laser system must be found for clinical use because scientists do not know the best laser and its parameters for neurosurgery. To find appropriate laser for the medical or surgical applications, laser-tissue interaction mechanism should be well understood. All biological tissues consist of mainly water that 65.3 percent of the tissues is water [4]. However, the percentage of the water varies that subcortical and cortical brain tissues consist of 72 percent and 82 percent water constituent, respectively [5]. For this reason, water constituent of the biological tissues is directly associated with the laser frequency choice in all medical applications [6, 7].

Up to now, many different lasers for each medical application have been used. For instance, Nd:YAG lasers emit at 1064 nm, penetrates more deeply than CO_2 laser and passes through water with little effect. This laser harms neural tissue because it scatters inside tissue. However, brain tumors are extremely vascularized, and Nd:YAG laser has a noticeable effect on the tumors [8]. CO_2 lasers have minimum scattering effect on tissues because it emits at 10600 nm, and in this region water has high absorption coefficient which leads to minimum scattering effect. Consequently, the most of CO_2 laser power is absorbed that it has very localized and intense thermal effect. This feature of CO_2 laser makes it a good cutting instrument [9]. Nevertheless, silica fibers are not suitable when wavelengths are longer than 2000 nm; therefore, in neurosurgery, lasers whose wavelengths lower than 2000 nm must be used [10]. CO_2 laser beam cannot be transmitted through optical fibers. This is a problem for minimally invasive surgeries (MIS) because more brain tumors exist inside of the brain. To reach these tumors, MIS is essential [4]. Besides, CO_2 laser are not be good option for tumor ablation due to vascularized tumor tissues [11]. On the other hand, Er:YAG lasers are not suitable for removal of brain tissue because it has sudden vaporization and cavitation effect on the brain tissue [12]. Argon ion lasers emit at 488 and 514 nm, and they are good coagulators [13]. This laser could be best coagulation application, but not removal of brain tumor tissues. 980 nm diode laser overlaps the water absorption peak in the near infrared region [11]. Approximately one decade ago, scientists carried out an investigation which is a stereotactic brain surgery in vivo with the 980 nm diode laser. They found that this laser has negligible thermal effect to the nearby tissue [14, 15]. Besides, 1940 nm thulium fiber laser has also absorption peak of water. In 1990, Nishroka et al. observed that the 2010-nm thulium laser has the lowest thermal effect to the healthy tissue than 2120-nm holmium laser [16]. Despite of thulium fiber lasers advantages in neurosurgery, investigations with this laser are very low.

In neurosurgery with lasers, the achievement of a laser treatment is associated with the reduction of thermal damage to the healthy tissue. Thermal damage results from sudden increase of imperfect temperature which leads to irreversible tissue damage and carbonization as CO_2 laser does [17, 18, 19, 20]. This can be achieved by a

detailed dose study to determine the optimal parameters which are mode of operation like pmm (pulsed-modulated-mode) and cm (continuous-mode), exposure time, laser output power, energy density, tissue type like cortical and subcortical tissue.

1.1 Aim of the Study

The objective of this investigation is to guide to select most favorable infrared laser for the neurosurgery. In the literature, numerous one-laser investigations exist for the brain ablation. However, there are not enough research which compares lasers for brain ablation in only one paper. For this reason, most suitable laser for the neurosurgery is not known in depth. In this investigation, four infrared lasers, which are 1940 nm thulium fiber laser, 1470 nm diode laser, 1070 nm ytterbium fiber laser and 980 nm diode laser, were operated with ex vivo lamb brain tissue to find appropriate parameters like mode of the operation, exposure time, energy density, type of tissue. Thermal damage is defined with ablated and coagulated areas. In this way, lowest thermal effect to the nearby healthy tissue was tried to found, and also optimum parameters were proposed for the clinical use.

2. BACKGROUND

2.1 Laser

LASER is an acronym of Light Amplification by Stimulated Emission of Radiation. A laser is an opto-electronic device that creates and amplifies a monochromatic, collimated and coherent light. Coherent, monochromatic and collimated features of a laser mean same phase, single wavelength and narrow light source, respectively. A laser device is generally supplied with other optical source whose energy higher than the laser output. In the literature, this phenomenon is described as pumping energy into amplifying medium. This medium is population inversion state which is the primary reason of lasers existence. When excitation mechanism pumps energy into the amplifying medium, each excited atom in it absorbs one photon; in this way, each excited atom emits two photons in same frequency, same direction and same phase due to the population inversion. This process give rise to the amplification of light. Active or amplifying medium has two mirrors in order to increase intensity of light. One of the mirror is totally reflected while the other is partially reflected, and mirrors supply positive feedback to active medium.

Using a laser in medicine gives many advantages when comparing to other techniques. Lasers are haemostatic, supply less postoperative pain, minimal scarring and swelling, reduce bleeding and operating time. However, lasers have risk of carbonization, collateral damage and preventing histological assessment. A laser can be classified as its frequency, output power, material of the amplifying medium and mode of operation. Today, many different type of lasers are used for different applications especially in medicine. Table 2.1 gives information of the laser classification [21].

Lasers have been widely used in medicine, scientific research, holography, communications and consumer products for approximately 50 years. Therefore, since it was invented, many different lasers have been manufactured, and especially in medical

Table 2.1
Laser Classification.

Parameter	**Classification**			
Frequency	IR	Visible		UV
Amplifying Medium	Gas	Solid State	Dye	Semiconductor
Power	Low Power		High Power	
Mode of Operation	Continuous Wave		Pulsed Wave	

science, lasers are used as not only a diagnostic tool but also a treatment method. These features of lasers make them popular. At the present time, engineers and scientists work on many potential lasers for future clinical use. Some lasers, which are used in medical science, are listed in Table 2.2 [11, 22].

2.2 Lasers in Neurosurgery

Diseases of the central nervous system(CNS) is associated with the neurosurgery. Treatment or surgery of brain tumors is very hard because nearly all of the tumors exist inside of the brain, not the surface on it, and also tumors might spread over all of the brain or exist in the brain piece by piece. In other words, tumor itself is not easily accessible [4], and complete and harmless tumor resection is almost impossible. Additionally, tumors might expand although physicians remove tumors. The reason is that they cannot remove all of the tumor tissue because identifying blurry boundary between tumor and healthy tissues during the operation is very hard. As a result, conventional surgical methods are not efficient [2].

Scientists have been interested in medical lasers for the neurosurgical use for approximately 40 years due to the capability of precise brain ablation, accessibility with optical fibers, lack of pain and coagulation features. The first laser in neurosurgery is a CO_2 laser [9]. However, CO_2 lasers are not appropriate for the coagulation of blood vessels. When the laser beam is applied, arteries and veins tend to bleed [4]. This is

Table 2.2
List of some medical lasers.

Laser	λ **[nm]**	**Water** μ_a	**Melanin** μ_a	**Hemoglobin** μ_a
KrF	248	0.0168	8600	586
XeCl	308	0.005	4800	307
XeF	351	0.002	2677	635
Argon ion	488-514	0.003	780	156
KTP	532	0.004	630	203
He-Ne	633	0.003	345	27
Dye/Diode	640	0.003	332	23
Dye/Diode	720	0.016	221	7
Dye/Diode	780	0.023	167	6
Diode	810	0.023	147	4
Diode	910	0.073	98	4
Diode	980	0.430	76	2
Nd:YAG	1064	0.120	57	
Ho:YAG	2120	27		
Er:YAG	2940	12000		
CO_2	10600	800		

unwanted situation especially in neurosurgery. On the other hand, an argon ion laser is not usable in neurosurgery because this laser beam scatters inside brain tissue, and also this laser needs 1000 times greater electricity than the CO_2 laser to achieve same output power. This causes expensive argon ion laser [23]. Moreover, Nd:YAG lasers are effective coagulation blood vessels. These lasers have been studied extremely. The first report on the clinical use of a Nd:YAG laser was given by Ascher et al. Ulrich et al. found that when Nd:YAG laser system which consists of 1319 nm laser and 200 μm fiber has good results on both ablation and coagulation. Er:YAG lasers with a wavelength of 2940 nm have limited thermal damage but effects the tissue mechanically. This laser beam vaporizes the soft tissues like brain suddenly; namely that this laser is not good in brain ablation [4]. Besides, Er:YAG laser cannot be used in MIS because

this laser beam cannot be transmitted with a fiber. Over 20 years, diode lasers which emits light in the near IR region have available. They are useful for medical use due to their portable size, longer operating time and lower cost. Diode laser beams absorbed into tissue due to the fact that diode lasers interact with melanin, darker pigments and hemoglobin [24].

Consequently, brain ablation with a laser has not been used efficiently in the clinic until now due to the lack of knowledge. In other words, scientists do not know which laser or lasers are appropriate for brain ablation, and which parameters of the laser such as exposure time, energy density, mode of operation and so on. More, as tissue type changes, the optical properties change, and this leads to different temperature increase. Besides, the absorption coefficient of water is not linear as the below Figure 2.1 [25]. All biological tissues consist of mainly water [4], so water content of biological tissues becomes an essential factor for laser choice [2, 3]. Moreover, brain tissues can be divided into two tissue types which are called as subcortical and cortical tissues. Subcortical tissues consist of 72 percent water constituent while water constituent of the cortical tissues are 82 percent [5]. To provide less thermal effect to the nearby healthy tissue is the most essential factor in the surgical operations. Therefore, one of the objective of this investigation is to find a laser which gives minimum thermal damage.

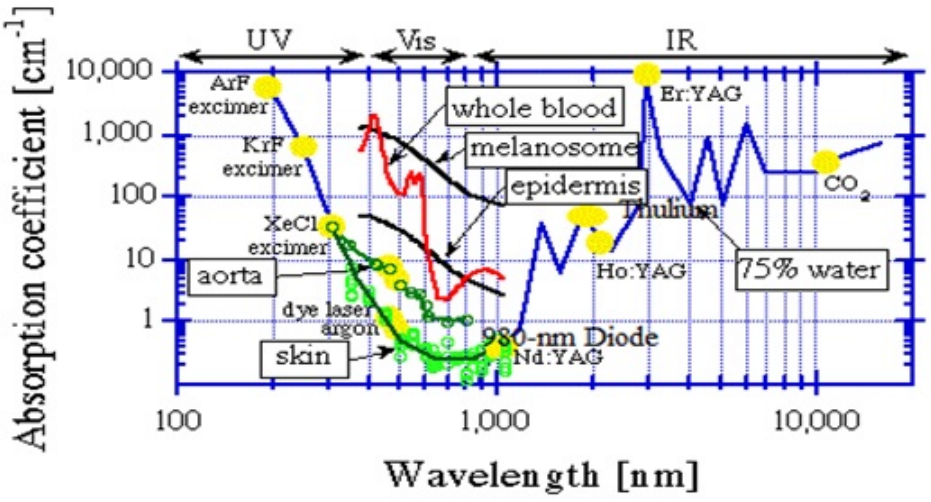

Figure 2.1 Absorption coefficient of water at some typical laser wavelengths.

2.3 Laser Tissue Interaction Mechanism

Since the invention of lasers, many investigations have been carried out potential interaction effects for all types of tissue targets and lasers. Today, there are five main interaction mechanisms which are photochemical interactions, photothermal interactions, plasma-induced ablation, photoablation and photodisruption. All these different interaction types are related to energy density, exposure time and wavelength of the laser. Map of these five basic interaction mechanisms are illustrated in Figure 2.2 [4]. In the chart, the ordinate shows the applied power density in W/cm^2 while the abscissa demonstrates the duration of laser exposure time in seconds; namely that exposure time and applied energy are very important parameters when selecting a certain type of interaction [4].

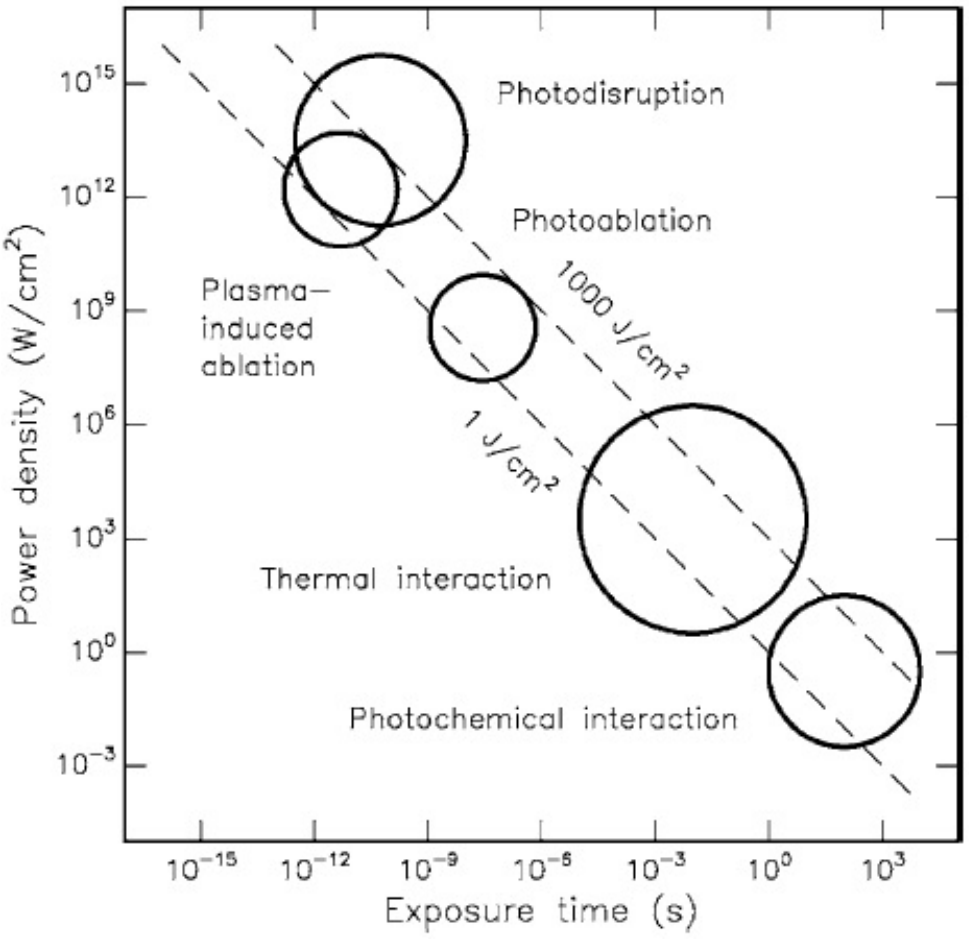

Figure 2.2 Map of laser-tissue interaction mechanisms.

2.3.1 Photothermal Interaction

When laser beam is applied to the tissue, local volumetric rate of heat production occurs [26]. Depending on the duration of the exposure time and the tissue temperature, different effects on the tissue might be observed. These effects are hyperthermia, coagulation, vaporization, carbonization and melting as illustrated in Figure 2.3 [4]. Besides, infrared lasers affects tissues thermally because they increase molecular vibrational activity.

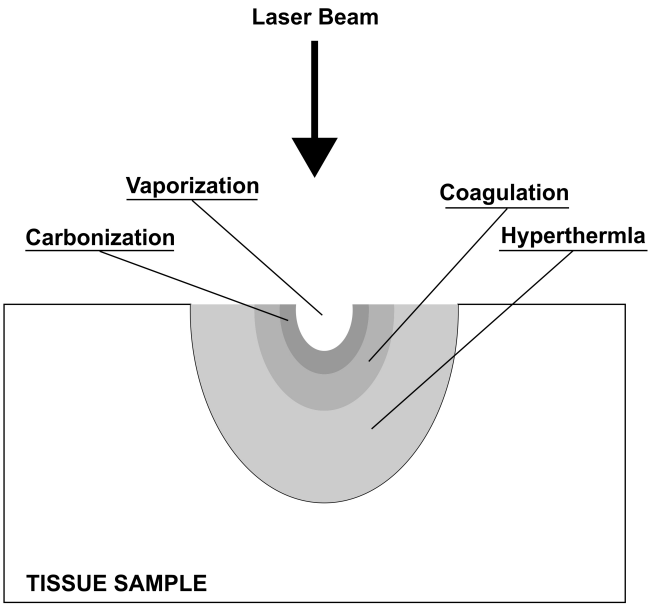

Figure 2.3 Photothermal effects of a laser.

2.3.1.1 Hyperthermia. Under normal circumstances, a body temperature is 37 °C, and there is no significant effect on the body up to 42 °C. When temperature of the tissue is increased up to 50 °C, bond destruction and membrane alterations occur. This phenomenon is called as hyperthermia, and it is reversible effect on the tissue. Beyond 50 °C, enzyme activities reduce, and repair mechanisms of the cell are disabled.

2.3.1.2 Coagulation. When temperature of tissue is reached up 60 °C, denaturation of collagen and proteins occurs. As a result, necrosis of cells and coagulation of tissue could be observed. When an infrared laser is applied on the tissue, coagulation generally comes into existence. This is thermal damage and irreversible effect, and it must be avoided in neurosurgery. Besides, coagulated tissue becomes necrotic.

2.3.1.3 Vaporization. Vaporization or ablation occurs when water molecules in tissues reach 100 °C. In neurosurgery, water is the main component in the brain. Therefore, vaporization can be seen generally. During vaporization, tissue expands in volume because of increased pressure; as a result, localized microexplosions occur. In the literature, vaporization is sometimes called as a thermomechanical effect because of the pressure build-up involved.

2.3.1.4 Carbonization. Above 100 °C, the local temperature of the target tissue dramatically increase and carbonization starts. Consequently, target tissue becomes black. For medical laser applications, carbonization should be avoided in any case [4]. To avoid carbonization, the tissue is cooled with gas or water during the operation.

2.3.1.5 Melting. At 300 °C, cracks and gas bubbles are observed especially on the tooth surface. The pulse duration of a few microseconds may be enough to enable a sufficient increase in temperature. All these temperature effects on the tissue are listed in Table 2.3 where the local temperature and the associated tissue effects are listed [4].

2.3.2 Photochemical Interaction

Photochemical interaction means that light can interact chemical effects and reactions within macromolecules or tissues as photosynthesis do. In the medical applications, photodynamic therapy (PDT) and biostimulation can be given as examples for photochemical interaction [4].

Table 2.3
Thermal effects of laser radiation.

Temperature	Biological effect
37 °C	Normal
45 °C	Hyperthermia
50 °C	Reduction in cell immobility and enzyme activity
60 °C	Denaturation of collagen and proteins, coagulation
80 °C	Permeability of membranes
100 °C	Vaporization and ablation
> 100 °C	Carbonization
> 300 °C	Melting

As seen from Figure 2.3, photochemical interaction mechanism exists at very low power densities and long duration of exposure time. The visible range like rhodamine dye lasers at 630 nm can be used in photochemical interaction because this range has high optical penetration depths.

During photodynamic therapy, a photosensitizer which has light-induced reactions is injected to a patient. After plenty of time, laser is irradiated to the subject. In this way, photosensitizers interact with unhealthy cells and they become necrosis. Therefore, the primary idea of photochemical treatment is to use a chromophore receptor acting as a catalyst. On the other hand, red and near infrared light sources such as helium-neon lasers can be used for biostimulation applications [4]. Studies on hair growth, wound healing and pain relief can be given as examples for biostimulation.

2.3.3 Photoablation

In photoablation, thermal damage like coagulation or vaporization does not come into existence due to the fact that UV laser beam breaks down the bonds of the macromolecule. Namely that UV lasers are used in the photoablation mechanism

which needs high power density.

2.3.4 Plasma-Induced Ablation

If power densities exceed $10^{11} W/cm^2$ in solids and fluids, optical breakdown occurs. It makes energy deposition possible in the pigmented tissue and weakly absorbing media [4].

2.3.5 Photodistribution

When breakdown takes place inside soft tissues such as a brain, cavitation and jet formation occur. Photodistribution needs high energy density like plasma-induced ablation mechanism. Besides, focusing the laser beam on the surface of the tissue or into it leads to cavitation effect [4].

3. MATERIALS

In this study, four infrared lasers are used to examine coagulation and ablation diameters on ex vivo lamb brain tissues which are subcortical and cortical tissues. In this way, most appropriate laser among them could be recommended for clinical use by calculating ablation efficiencies. These infrared lasers are 1940-nm thulium fiber laser or Tm:YAP laser, 1470-nm diode laser, 1070-nm ytterbium fiber laser or Nd:YLF and 980-nm diode laser. All of them have different output power and effect on biological matters due to their absorption coefficients for water molecules. Laser power was carried through two 400-μm silica coated optical fibers. These are manufactured by Spindler-Hoyer and OZ Optics companies. Spindler-Hoyers optical fiber was used in experiments with Tm:YAP and Nd:YLF laser devices. Other optical fiber was used with 1470-nm and 980-nm diode laser. These optical fibers are showed in Figure 3.1. Besides, before and during every experiment, optical laser tip was cleaned with a sandpaper by using a SMA connector (Opto Power OPC-OC-01, Opto Power Corporation, Tuscon, AZ, USA), and also tip is controlled with a magnifying glass. This mechanism is showed in Figure 3.2.

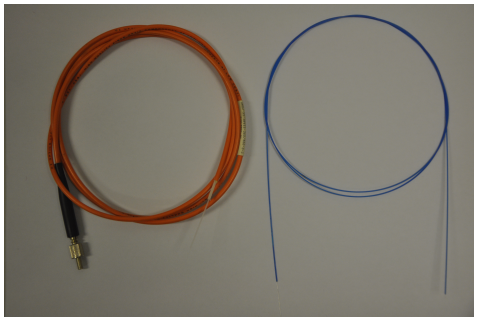

Figure 3.1 Optical fibers (right-hand side and left-hand side are from OZ Optics Ltd. and Spindler-Hoyer, respectively).

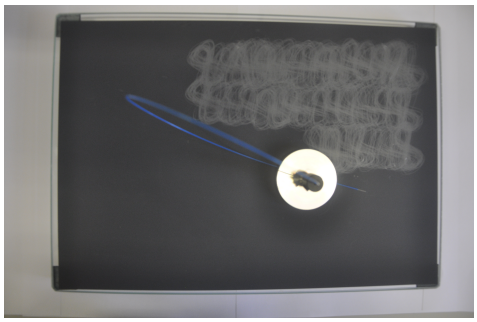

Figure 3.2 Cleaning materials (sandpaper, SMA connector and magnifying glass) for optical fiber tips.

3.1 Experimental Setup

3.1.1 1940-nm Thulium Fiber Laser System

1940-nm thulium fiber laser system consists of 1940-nm Tm:YAP (Thulium-doped Yttrium Aluminum Garnet) laser device, a microcontroller unit (Teknofil Ltd., Istanbul, Turkey), a power meter (Newport Corporation, Model: 1918C, Bozeman ,MT, USA), a power meter detector (Newport Corporation, Model No: 818P-030-19), silica coated optical fiber with 400-μm (Spindler-Hoyer, Göttingen, Germany), opto-mechanic devices (Thorlabs, USA), an eyewear (Sperian Protection Inc.), and a PC based user interface program of thulium fiber laser modulation controller (LaserMod.vi, Teknofil Ltd., Istanbul, Turkey) as seen in Figure 3.3 and Figure 3.4.

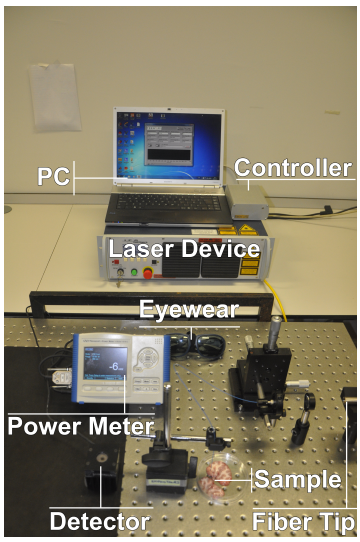

Figure 3.3 Experimental setup of Tm:YAP fiber laser system.

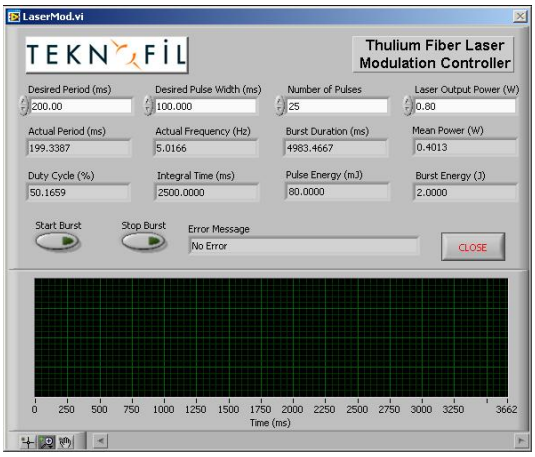

Figure 3.4 User interface of Tm:YAP fiber laser system.

Manufacturer of the laser device is IPG Photonics GmbH, Burbach, Germany, and its model and serial numbers are TLR-5-1940 and 9050721, respectively. This device has 5 W maximum average power. Power cannot be arranged by the user interface but buttons of the laser device can enable this. However, duration of pulsed wave on-off time is easily arranged by the user interface. The tissue was exposed with a 400-μm silica coated optical fiber (Spindler-Hoyer, Göttingen, Germany). The optical powermeter was used so as to check the output power frequently during the experiment. When the output power deviated or tip of the fiber was damaged, essential adjustments were done.

3.1.2 1470-nm Diode Laser System

This setup consists of a diode laser device (12/400-1470-1H10.1, DILAS, Mainz, Germany), a power meter (Newport Corporation, Model: 1918C, Bozeman ,MT, USA), a power meter detector (Newport Corporation, Model No: 818P-030-19), 400-μm silica coated optical fiber(OZ Optics Ltd., 613.831.0981, Canada), an eyewear (Sperian Protection Inc.), and a PC based user interface program as seen in Figure 3.5 and Figure 3.6. A microcontroller is not necessary in this setup due to the fact that continuous mode, duration of pulse width and laser output power can be easily adjusted via PC based interface which is called as DL-System MINI. 1470-nm diode laser gives maximum output power of 12W, and this power is changed via user interface program.

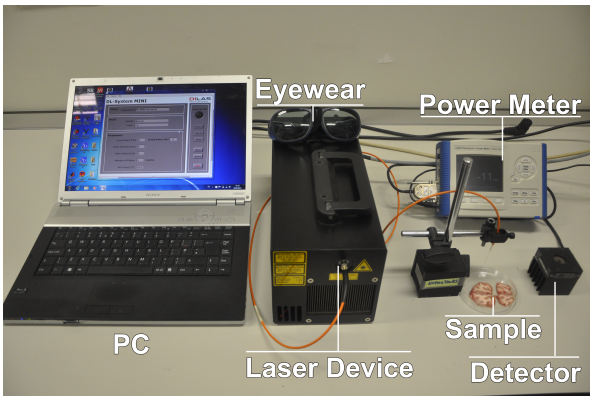

Figure 3.5 Experimental setup of 1470-nm diode laser system.

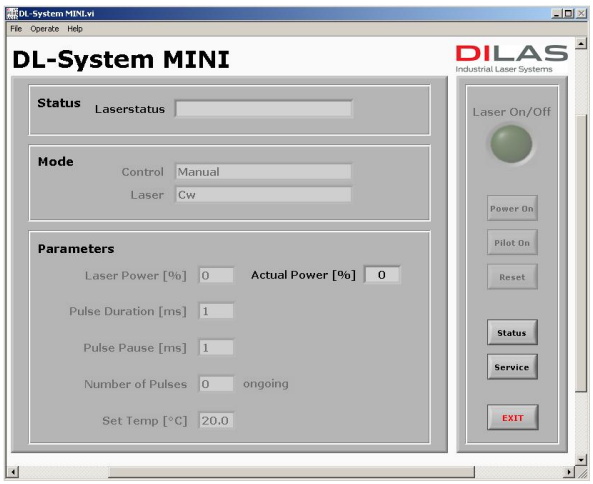

Figure 3.6 User interface of 1470-nm diode laser system.

3.1.3 1070-nm Ytterbium Fiber Laser System

There are some devices in 1070-nm ytterbium fiber laser system such as Nd:YLF laser device (7032621, IPG Laser GmbH, Burbach, Germany), a microcontroller (designed and produced in biophotonics laboratory, BME, Bogazici University, Istanbul, Turkey), a power meter (Newport Corporation, Model: 1918C, Bozeman ,MT, USA), a power meter detector (Newport Corporation, Model No: 818P-030-19), 400-μm silica coated optical fiber(Spindler-Hoyer, Göttingen, Germany), opto-mechanic devices (Thorlabs, USA), an eyewear (Sperian Protection Inc.). There is no any interface program but cm execution time or pulse width can be obtained by the microcontroller. However, laser output power is adjusted by using the laser device. Besides, the maximum average output power is 20W. This setup is showed in Figure 3.7.

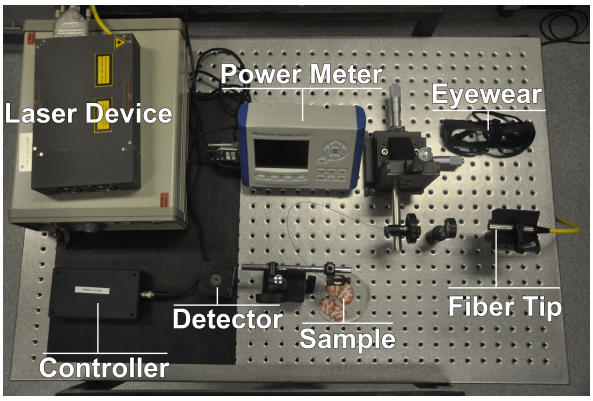

Figure 3.7 Experimental setup of Nd:YLF fiber laser system.

3.1.4 980-nm Diode Laser System

Eventually, this system has a 980-nm diode laser device (OPC-D010-980-FCPS, Serial No: P9711-379, Opto Power Corp., AZ, USA), SMA connector to connects the laser fiber tip with optical fiber (Opto Power OPC-OC-01, Opto Power Corp., AZ, USA), a microcontroller device (Teknofil Ltd., Istanbul, Turkey), a power meter (Newport Corporation, Model: 1918C, Bozeman ,MT, USA), a power meter detector (Newport Corporation, Model No: 818P-030-19), 400-μm silica coated optical fiber(OZ Optics Ltd., 613.831.0981, Canada), an eyewear (Sperian Protection Inc.), and a PC based user interface program. The laser output power is 10W. This system and the user interface can be seen in Figure 3.8 and Figure 3.9, respectively.

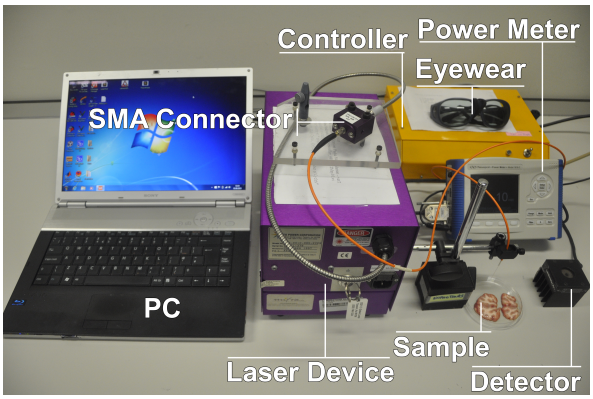

Figure 3.8 Experimental setup of 980-nm diode laser system.

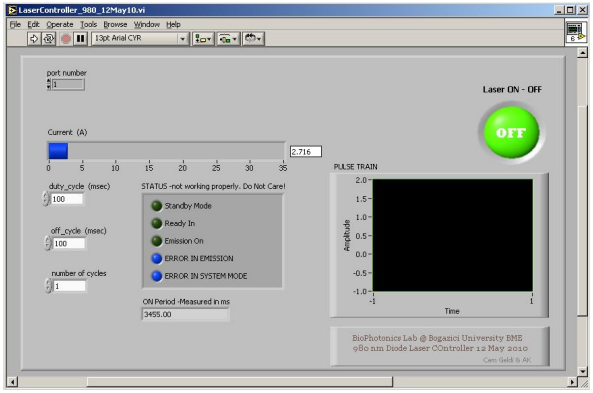

Figure 3.9 User interface of 980-nm diode laser system.

3.2 Sample Collection

For both pre-dosimetry and dosimetry studies, totally 60 fresh lamb brains which weigh 55-70 g were used. After a lamb was sacrificed within 24 hours, experiments were conducted. As reported in literature [27], the lamb brain samples were cooled to (4 °C) and stored in 100 percent humidity to prevent tissue degradation. Before the laser application, the lamb brain temperature was raised to the room temperature (22 °C). After the experiment the brain samples were not be used again and again, and also not-fresh lamb brain samples were not be utilized. The diameters of the lamb brain is $10.00 \pm 0.4 \times 7.5 \pm 0.2 \times 3 \pm 0.2$ cm as seen in Figure 3.10.

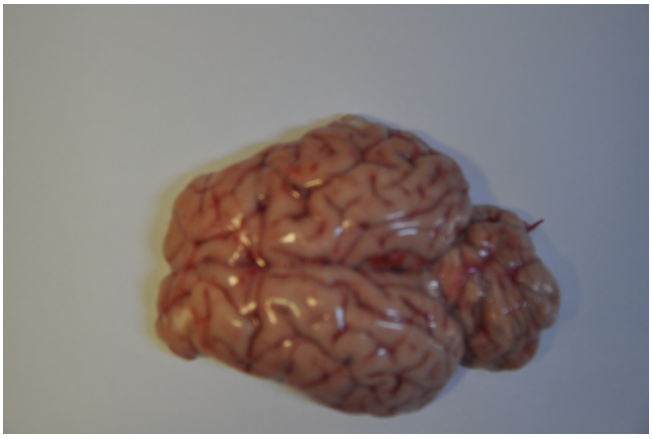

Figure 3.10 Lamb brain tissue.

3.3 Equipment

1. Laser : 1940-nm Thulium Fiber Laser System, TLR-5-1940, IPG Photonics GmbH, Burbach, Germany.
2. Laser : 1470-nm Diode Laser, 12/400-1470-1H10.1, DILAS, Mainz, Germany.
3. Laser : 1070-nm Ytterbium Fiber Laser System, 7032621, IPG Photonics GmbH, Burbach, Germany.
4. Laser : 980-nm Diode Laser, OPC-D010-980-FCPS, Opto-Power Corp., AZ, USA.
5. SMA Connector : Opto-Power OPC-OC-01, Opto-Power Corp., AZ, USA
6. Power Meter : 1918C, Newport Corporation, Bozeman, MT, USA.
7. Power Meter Detector : 818P-030-19, Newport Corporation, Bozeman, MT, USA.
8. Laser Safety Glasses : Sperian Protection Inc.
9. Optical Fiber : 400-μm Silica Coated, 613.831.0981, OZ Optics Ltd., Canada.
10. Optical Fiber : 400-μm Silica Coated, Spindler-Hoyer, Göttingen, Germany.
11. Microscope : H550L, Nikon Corporation, Japan.
12. Microcontroller : Microcontroller unit of 1940-nm Thulium Fiber Laser System, Teknofil Ltd., Istanbul, Turkey.
13. Microcontroller : A microcontroller unit of 1070-nm Ytterbium Fiber Laser System BME, BOUN, Istanbul, Turkey.
14. Microcontroller : A microcontroller unit of 980-nm Diode Laser, Teknofil Ltd., Istanbul, Turkey.
15. Opto-Mechanic Devices : Thorlabs, USA.

4. METHODS

After lamb brain samples reach to the room temperature (22 °C), brain was cut coronally. In this way, laser application could be done on each approximately 6-7 mm thick coronal section, and other dimensions were $6.00 \pm 0.4 \times 3.5 \pm 0.2$ cm. Laser beam was radiated towards midline of the samples, and also in all of the experiments two type of brain tissues were used. These tissues are called as subcortical and cortical tissues. During the experiment, tissue were enveloped with saline so as to hinder the sample to dehydrate. Lamb brain tissue is showed in Figure 4.1. In the pre-dosimetry study, total 1280 laser shots were conducted. Data was gathered for all two tissue structures which are cortical and subcortical. In other words, 1940-nm, 1470-nm, 1070-nm and 980-nm lasers radiated 400 times, 280 times, 400 times and 200 times, respectively. Besides, 1280 laser shots were achieved during the dosimetry study. In the dosimetry study, each laser emitted 320 shots (160 shots for cm and other 160 shots for pmm). Each laser generated 4 laser output levels and 2 energy densities. This distribution for each laser system is illustrated in Table 3.1, Table 3.2, Table 3.3 and Table 3.4. Besides, each laser dose was performed 10 times for each cortical and subcortical tissues.

In pulsed-modulated wave, one cycle is 200 milliseconds, and both on and off durations are 100 milliseconds. These values were applied to all experiments. On-off duration can be controlled by the controller units with PC based interface programs for 1980-nm thulium fiber laser and 980-nm diode laser. 1470-nm diode laser uses only an interface program that every steps can be adjusted like 980-nm and 1940-nm lasers. However, 1070-nm ytterbium fiber laser uses a controller device which designed and produced by our biophotonics team. Before and after each application, laser power is controlled with an optical powermeter. Besides, silica coated optical fiber tip was checked for irregularities and cleaned when carbonization or damage occurred on the tip.

Before the dosimetry study, pre-dosimetry study was conducted for all lasers

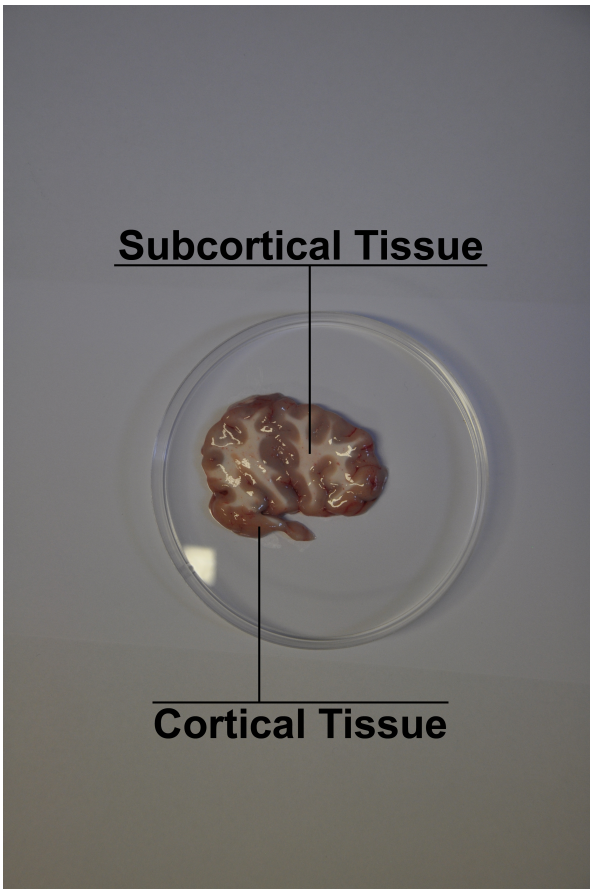

Figure 4.1 Lamb brain tissue: subcortical and cortical tissues.

in order to obtain the parameters for both subcortical and cortical tissues. In this way, carbonization and coagulation onset times were obtained by raising power 100 mW increments from 100 mW up to 1000 mW for 1940-nm thulium fiber laser. For 1470-nm diode laser, 250mW increments from 500 mW to 2,500 mW are applied. In 1070nm ytterbium fiber laser application, data was collected form 500 mW to 5000 mW with 500 mW increments. Eventually, 1W−5W with 1 W increments was done in 980-nm diode laser application. In this way, safe ablation and coagulation regions for both cm and pmm were obtained for dosimetry study. In both modes, pulse widths and laser power were chosen so as to provide same amount of energy ($2 - 4$ J or $20 - 40$ J)to the both brain tissues.

After pre-dosimetry study, dosimetry study was applied for all lasers with cm and pmm on not only cortical tissue but also subcortical tissue. Exposure time was defined with results of the pre-dosimetry study. After irradiation of laser light, tis-

sue is measured under a microscope (H550L, Nikon Corporation, Japan). In this way, ablation diameters and coagulation diameters could be obtained by using PC based program which is called as NIS-Elements Documentation. Data acquisition setup is showed in Figure 4.2, and also ablation and coagulation diameters with a brain tissue sample is demonstrated in Figure 4.3. It is purposed to find the suitable laser parameters so as to obtain best ablation efficiency and minimum damage. Ablation efficiency can be calculated as:

$$AblationEfficiency = \frac{AblationDiameter}{CoagulationDiameter} \times 100 \tag{4.1}$$

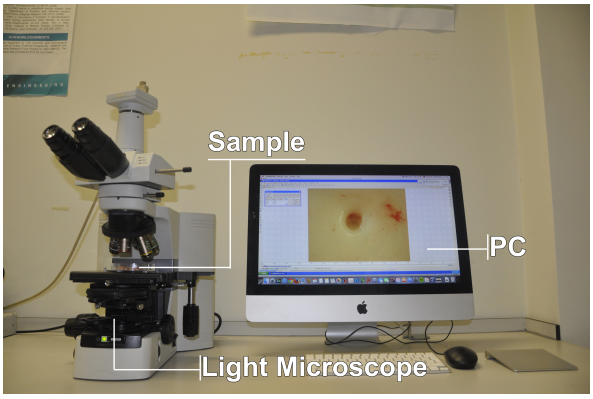

Figure 4.2 Data acquisition setup.

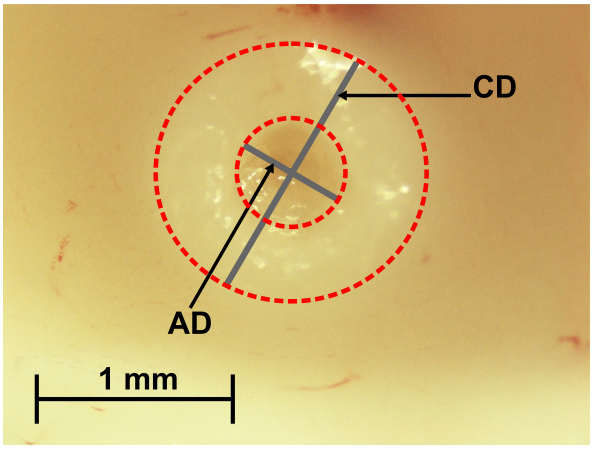

Figure 4.3 A brain tissue sample. CD: coagulated tissue diameter, AD: ablated tissue diameter.

Table 4.1
Dosimetry levels for 1940-nm thulium fiber laser.

Mode	**Laser Power[W]**	**Intensity[W/cm^2]**	**Duration[sec]**	**Energy[J]**
cm	0.2	0.157	10	2
cm	0.2	0.157	20	4
cm	0.4	0.314	5	2
cm	0.4	0.314	10	4
cm	0.6	0.472	3.33	2
cm	0.6	0.472	6.67	4
cm	0.8	0.630	2.5	2
cm	0.8	0.630	5	4
pmm	0.2	0.157	20	2
pmm	0.2	0.157	40	4
pmm	0.4	0.314	10	2
pmm	0.4	0.314	20	4
pmm	0.6	0.472	6.67	2
pmm	0.6	0.472	13.34	4
pmm	0.8	0.630	5	2
pmm	0.8	0.630	10	4

Table 4.2
Dosimetry levels for 1470-nm diode laser.

Mode	**Laser Power[W]**	**Intensity[W/cm^2]**	**Duration[sec]**	**Energy[J]**
cm	0.5	0.393	4	2
cm	0,5	0.393	8	4
cm	1	0.787	2	2
cm	1	0.787	4	4
cm	1.5	1.18	1.33	2
cm	1.5	1.18	2.67	4
cm	2	1.574	1	2
cm	2	1.574	2	4
pmm	0.5	0.393	8	2
pmm	0.5	0.393	16	4
pmm	1	0.787	4	2
pmm	1	0.787	8	4
pmm	1.5	1.18	2.67	2
pmm	1.5	1.18	5.34	4
pmm	2	1.574	2	2
pmm	2	1.574	4	4

Table 4.3
Dosimetry levels for 1070-nm ytterbium fiber laser and 980-nm diode laser.

Mode	**Laser Power[W]**	**Intensity[W/cm^2]**	**Duration[sec]**	**Energy[J]**
cm	1	0.787	20	20
cm	1	0.787	40	40
cm	2	1.574	10	20
cm	2	1.574	20	40
cm	3	2.36	6.67	20
cm	3	2.36	13.34	40
cm	4	3.15	5	20
cm	4	3.15	10	40
pmm	1	0.787	40	20
pmm	1	0.787	80	40
pmm	2	1.574	20	20
pmm	2	1.574	40	40
pmm	3	2.36	13.34	20
pmm	3	2.36	26.67	40
pmm	4	3.15	10	20
pmm	4	3.15	20	40

5. RESULTS AND DISCUSSION

Pre-dosimetry studies are essential tools to guide to find the best results, and to determine carbonization time and the parameters for continuous and pulsed-modulated modes. Carbonization occurs when the temperature of the tissue passes threshold of 100 °C. It must be avoided. Besides, coagulation of tissue is the first sign, and ablation occurs after it. Therefore, coagulation and carbonization onset times were recorded in the pre-dosimetry study. In this way, the safe interval times for lamb brain tissue were recorded, and illustrated in the following graphs.

Pre-dosimetry studies for all lasers which are 1940-nm thulium fiber laser, 1470-nm diode laser, 1070-nm ytterbium fiber laser and 980-nm diode laser were done one by one. Because of different absorption coefficients for water through the spectrum, laser effect on brain tissue is different. It causes that different laser beams penetrate different distances into the tissue, and this feature of the lasers is their success in medical applications like different tissue removal. In other words, when 500mW power is applied with thulium fiber laser, coagulation time on the brain tissue is lower than the other laser application which uses 1070-nm ytterbium fiber laser and same amount of power. Moreover, some power levels cannot generate any carbonization at least up to 4 minutes. Therefore, carbonization onset times are not showed due to their absence up to 240 seconds.

After pre-dosimetry study, dosimetry study was carried out. The power levels and exposure time were defined under the results of the pre-dosimety study. There are totally 16 graphs which are combination of four output powers, two energy densities, two type of brain tissues (cortical and subcortical), two operation modes (continuous and pulsed-modulated modes) and four laser devices. In this way, comparison of at least infrared lasers on ex vivo lamb brain tissues would be obtained, and ablation efficiencies of these laser beams on the brain tissue would be discussed.

For pre-dosimetry studies as well as dosimetry studies, 10 laser shots were applied on not only cortical but also subcortical tissues for each power level. Silica laser tip was vertically approached to the surface of the both tissues. Distance between the silica laser tip and the surface of the tissue is 0-3 mm. Before each experiment, silica laser tip was cleared for deformities.

5.1 Data Analysis

In the pre-dosimetry and dosimetry studies, statistical analysis was conducted to reveal the impacts of parameters. Besides, statistical differences were determined for diameters of ablation and coagulation and the onset times. In the data analysis, ANOVA test was used with Tukey test, and also significant level was determined as $P<0.05$.

In the pre-dosimetry study, totally 85 groups were created. 1940-nm Tm:fiber laser, 1470-nm diode laser, 1070-nm ytterbium fiber laser and 980-nm diode laser were divided into 24, 25, 20 and 16 groups, respectively. The number of the groups for each laser system do not equal because there are different power levels for each laser application, and also any group is beside the point when there is no carbonization onset time. In this study, carbonization and coagulation onset times are differentiated with tissue type ($P<0.001$), wavelength ($P<0.001$) and laser output power ($P<0.001$). Variations of different tissue type, wavelength and laser power cause different onset times.

In the dosimetry study, totally 192 groups were created for four laser system. Both Tm:fiber laser and 1470-nm diode laser applications were divided into pair of 64 groups, and also pair of 32 groups were generated for the other two applications. It was found that coagulated tissue diameter and ablated tissue diameter were differentiated with 5 parameters: laser output power ($P<0.001$), wavelength ($P<0.001$), tissue type ($P<0.001$), mode of operation ($P<0.001$), energy density ($P<0.001$). Variations of the different laser output power, wavelength, tissue type, mode of operation and energy

density result with remarkable changes within both diameters. However, there are some exceptions for some of the laser applications that are defined in the relevant sections.

5.2 Pre-Dosimetry Study

5.2.1 1940-nm Thulium Fiber Laser System

1940-nm thulium fiber laser has the highest absorption coefficient for among four lasers. Hence, it has minimum scattering effect and maximum penetration depth on the brain tissues. In the pre-dosimetry studies, onset times of coagulation and carbonization were obtained by raising power by 100 mW increments up to 1000 mW. However, local explosion on both brain tissues occurs due to sudden temperature increase after 800mW; therefore, carbonization onset times for 900 mW and 1000 mW are not be showed. These durations (carbonization and coagulation onset times) were visually inspected, and both brain tissues were examined. Besides, 10 laser shots were applied for each laser power and brain tissue.

In subcortical tissue examination, there is no carbonization time (at least up to 240 seconds) up to 500 mW. After this power, carbonization starts, and onset time of it decreases as output power is increased as seen in Figure 5.1 ($P<0.001$). The cortical tissue was exposed with same amount of power as seen in Figure 5.2. In this investigation, carbonization onset time starts at 500 mW but carbonization onset time in cortical tissue is bigger than the subcortical one ($P<0.001$). This can be explained that subcortical and cortical tissues do not have same amount of water [5]. Again, there is no carbonization onset time (at least up to 240 seconds) up to 400 mW for the cortical tissue. Consequently, as laser power is increased, onset times decrease, and there is no carbonization time up to 500 mW ($P<0.001$).

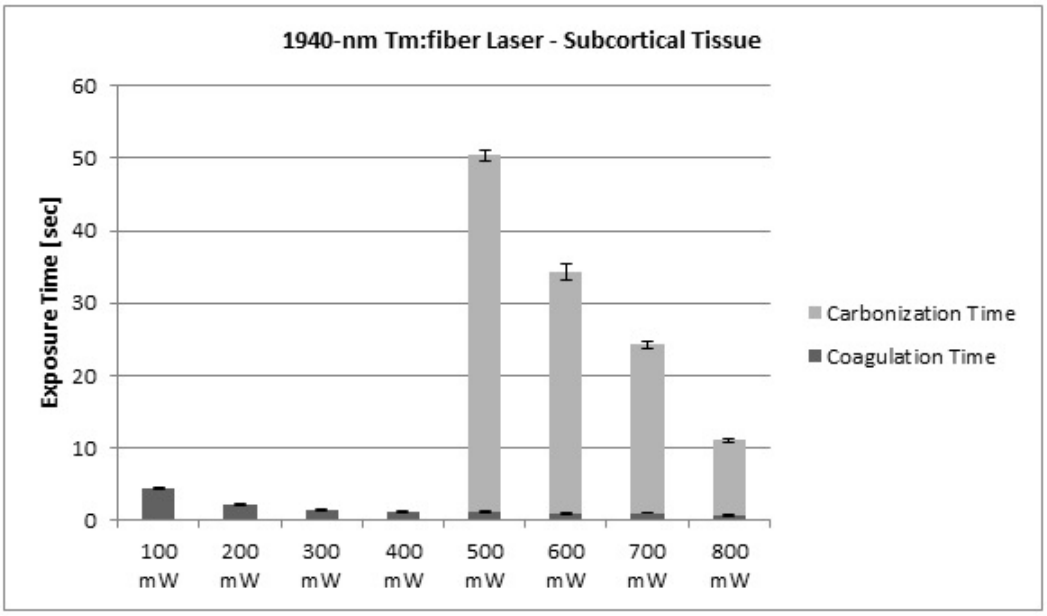

Figure 5.1 Carbonization and coagulation onset times versus laser output power of 1940-nm Tm:fiber laser on the subcortical tissue.

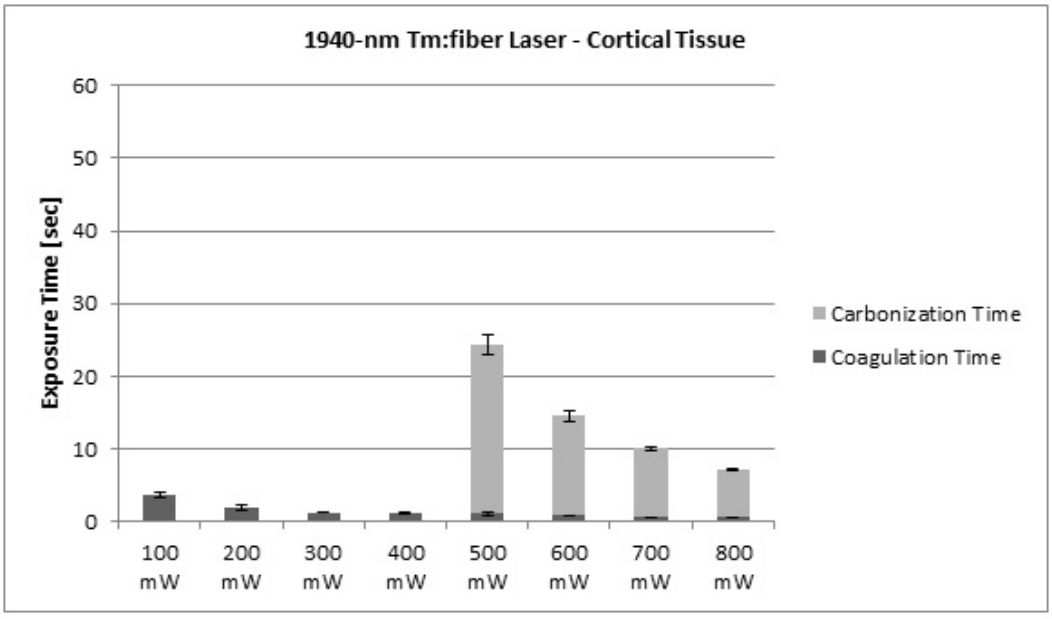

Figure 5.2 Carbonization and coagulation onset times versus laser output power of 1940-nm Tm:fiber laser on the cortical tissue.

5.2.2 1470-nm Diode Laser System

1470-nm diode laser device, which has the second highest absorption coefficient value among all lasers, were used in the study. Carbonization and coagulation onset

times were recorded like 1980-nm thulium fiber laser. Again, total 280 laser shots were applied for the combination of both tissue types all power levels. Carbonization and coagulation onset times are illustrated for subcortical and cortical tissues in Figure 5.3 and Figure 5.4, respectively. Cortical tissue would have less carbonization onset time because it has less water constituent than the subcortical one. However, carbonization onset time is bigger for cortical tissue after 1 W due to the fact that cortical tissue is exploded locally after laser power at 1 W which leads to higher carbonization onset time ($P<0.001$). Besides, duration carbonization and coagulation onset times for same amount of power output are bigger for this laser when comparing with 1940-nm thulium fiber laser ($P<0.001$). This is expected case because 1940-nm thulium fiber laser has minimum scattering effect on the brain tissue; therefore, laser beam of the 1940-nm thulium fiber laser become more intense on the brain tissue. For example, carbonization time on the cortical tissue begins at 10 and 80 seconds for 1940-nm Tm:fiber (at 700 mW) and 1470-nm diode lasers (at 750 mW), respectively. On the other hand, there is no any carbonization onset times up to 0.75 W and 1 W for subcortical and cortical tissues, respectively.

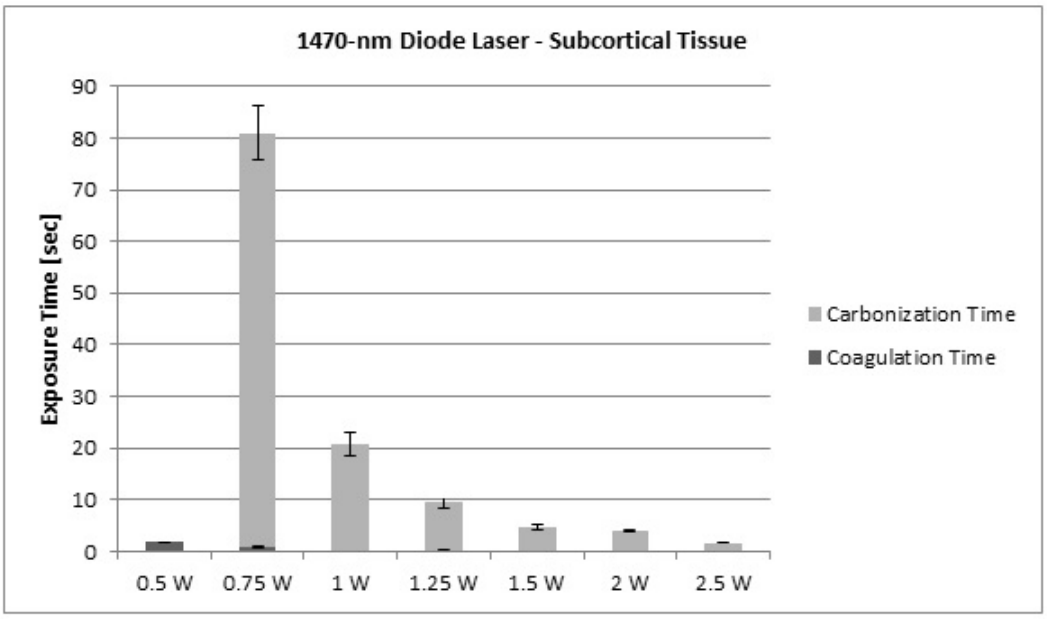

Figure 5.3 Carbonization and coagulation onset times versus laser output power of 1470-nm diode laser on the subcortical tissue.

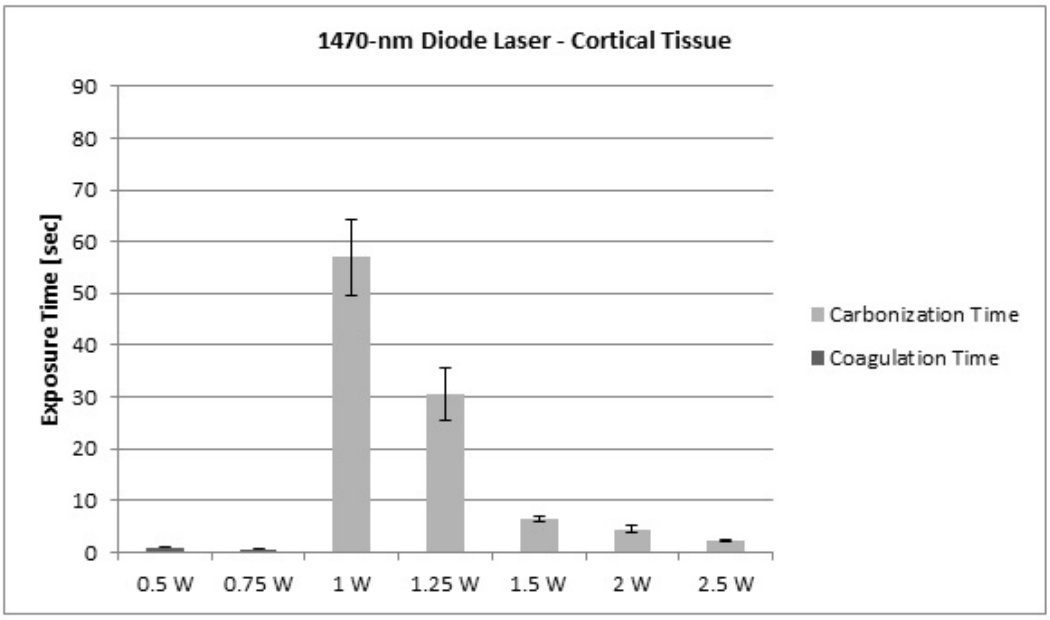

Figure 5.4 Carbonization and coagulation onset times versus laser output power of 1470-nm diode laser on the cortical tissue.

5.2.3 1070-nm Ytterbium Fiber Laser System

Third pre-dosimetry study is 1070-nm ytterbium fiber laser. This laser has the minimum absorption coefficient among four infrared lasers. Therefore, temperature of the tissue cannot reach to 100 °C that leads to never carbonization effect or ablation effect on the tissue at least up to 4 minutes. Therefore, carbonization onset time cannot be showed. In this study, onset times of coagulation and carbonization for both tissues were obtained by raising power by 0.5 W increments up to 5 W. Totally, averages of the 200 laser shots were illustrated in Figure 5.5 and Figure 5.6. Cortical tissue has more water component with 82 percent than subcortical tissue with 72 percent [5]. For this reason, duration of coagulation time for subcortical tissue is bigger than the cortical tissue. Moreover, coagulation onset times decrease as the power is increased ($P<0.001$).

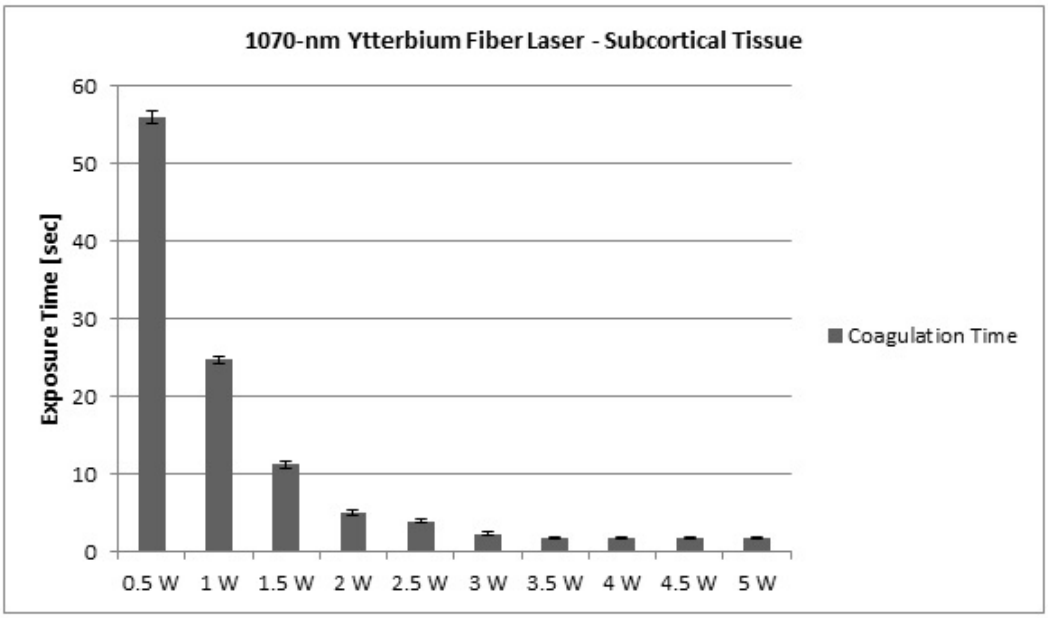

Figure 5.5 Coagulation onset time versus laser output power of 1070-nm ytterbium fiber laser on the subcortical tissue.

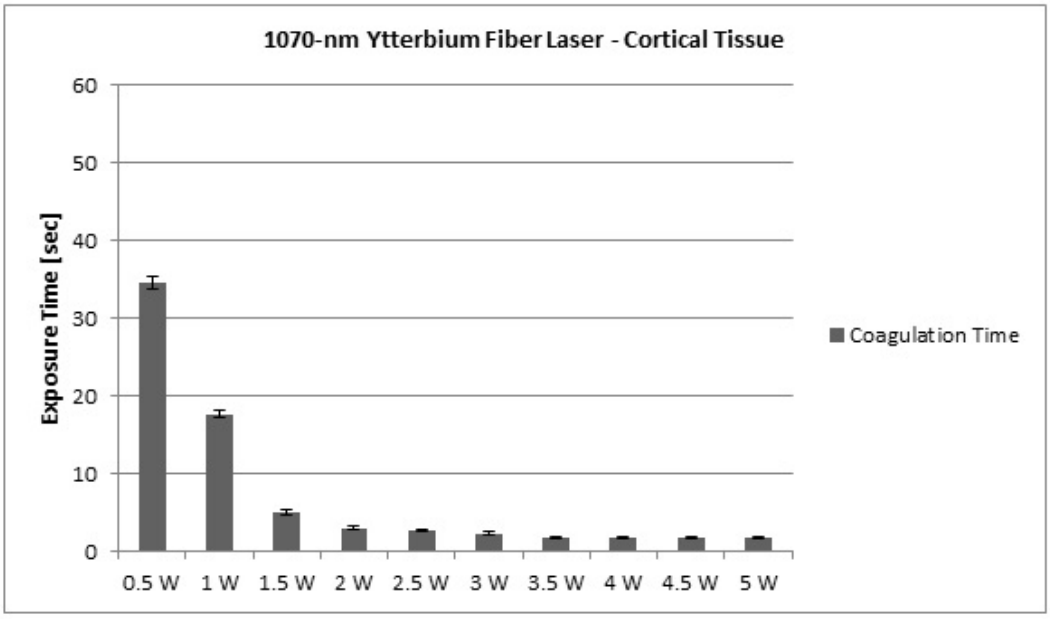

Figure 5.6 Coagulation onset time versus laser output power of 1070-nm ytterbium fiber laser on the cortical tissue.

5.2.4 980-nm Diode Laser System

Wavelength of the 980-nm diode laser is lower than the 1070-nm ytterbium fiber laser. However, this laser should be noted as a special case that it has a local peak in the water absorption coefficient in the near infrared region [14]. As a result, it has carbonization onset time for some of the power outputs but 1070-nm ytterbium fiber laser does not have any carbonization onset time. In this pre-dosimetry study, total 200 laser shots were applied on not only cortical tissue but also subcortical tissue. Data was obtained by raising power by 1 W increments up to 5 W as seen in Figure 5.7 and Figure 5.8. Carbonization onset time was not recorded till 3 W, and maximum duration of laser radiation was adjusted till 240 seconds. Again, cortical tissue has the lower onset times than the other tissue type due to different water densities in cortical and subcortical tissues ($P<0.001$).

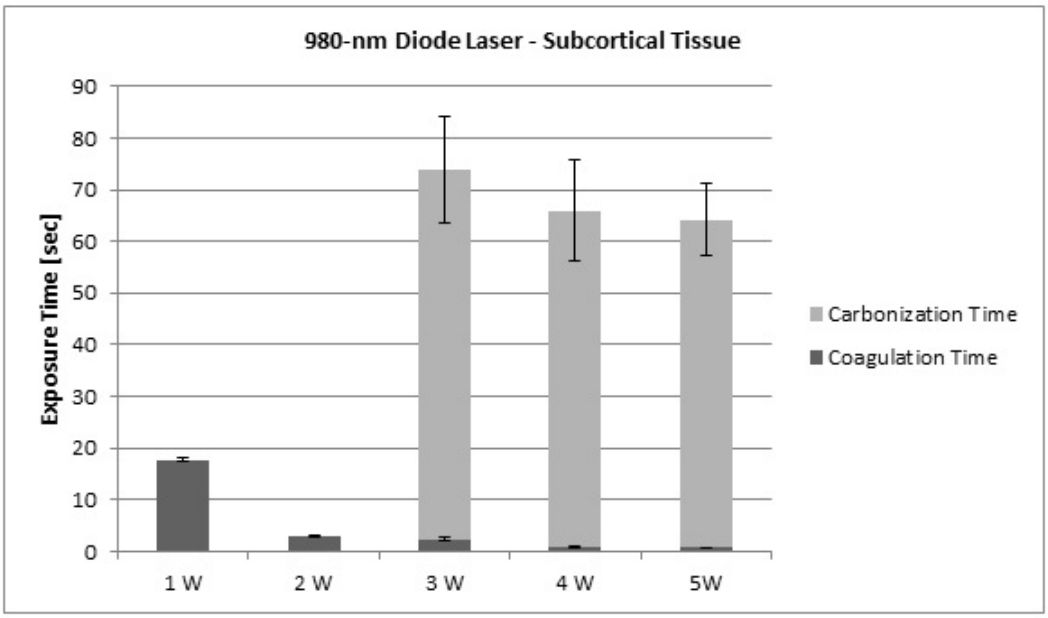

Figure 5.7 Coagulation onset time versus output power of 980-nm laser on the subcortical tissue.

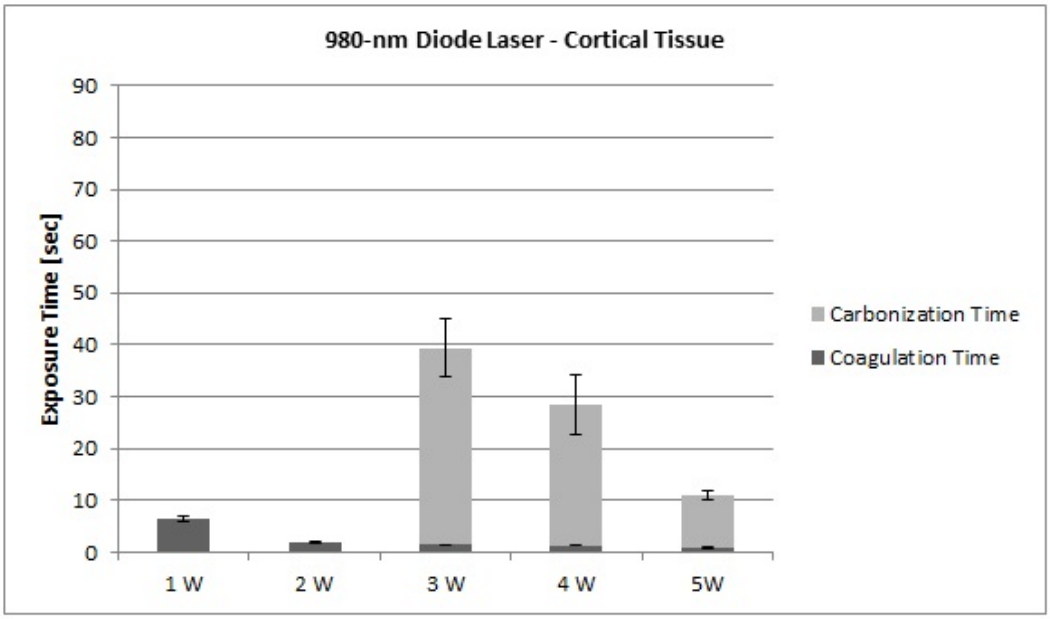

Figure 5.8 Coagulation onset time versus output power of 980-nm laser on the cortical tissue.

Consequently, different laser power levels were applied for each application in the pre-dosimetry study. For instance, up to 1 W laser radiation for 1940-nm Tm:fiber laser application was recorded while up to 5 W laser emission for 1070-nm ytterbium fiber laser application was applied. 1940-nm Tm:fiber laser has maximum absorption coefficient while 1070-nm ytterbium fiber laser has minimum absorption coefficient. Moreover, the wavelength of the 980-nm diode laser is minimum value among four lasers but it does not have minimum absorption coefficient because local peak in the absorption coefficient of water makes this laser an exception in this region. Therefore, carbonization onset time was not recorded for 1070-nm ytterbium fiber laser while carbonization onset time was observed after 3 W laser power in both tissues in the 980-nm diode laser application. In general, onset times for 1940-nm Tm:fiber laser is more less but it cannot be easily compared with other lasers graphs due to different power outputs ($P<0.001$). However, when other last three lasers are compared at same amount of power density, it is obvious that coagulation onset time is higher for 1070-nm ytyerbium fiber laser, and lower for the 1470-nm diode fiber laser for both tissue types at 1 W laser power output ($P<0.001$). This is expected that this onset times are directly related to the water absorption coefficients and proportion of water molecules.

Proportion of water in tissues influences the onset times. For example, subcortical tissue has more proportion of water that leads to less onset time because laser beam interacts with water further. Moreover, the pre-dosimetry study was conducted visually; therefore, onset times are in some degree bigger during observations for subcortical tissues because structural changes on the subcortical tissue like coagulation cannot be easily recognized due to its color. However, coagulation onset time for cortical tissue can be distinguished easily because it is brown and when it is coagulated, color of the cortical tissue changes which is easy to observe visually.

5.3 Dosimetry Study

Objective of the dosimetry study is to examine potential laser device for the neurosurgery. Therefore, impact of the four IR lasers on the lamb brain tissue was investigated and compared. In this study, different parameters like duration of exposure time, laser output power, energy density, and operation modes (cm and pmm) were investigated and ablation efficiencies (diameter of removed tissue over diameter of the total photothermal damage) were found for ex vivo lamb brain tissues.

In the 1940-nm thulium fiber laser application and 1470-nm diode laser application, energy densities of 2 J and 4 J were applied to the lamb brain tissues. However, energy densities of 2 J and 4 J is not sufficient to generate a lesion in the brain by using 1070-nm ytterbium fiber laser and 980-nm diode laser. Therefore, 10 times bigger energy densities (20 J and 40 J) were used in the last two applications. In this way, diameters of coagulation and ablation areas were calculated under the light microscope (Eclipse 80i, Nikon Corp., Japan) via a program (NIS Elements-D, Nikon Co.). Besides, 10 laser shots were applied to the both tissues in each laser applications. It is purposed to find suitable laser parameters so as to find maximum ablation efficiency which is obtained as the ratio of diameter of the ablation area to the diameter of the total thermally altered area.

5.3.1 1940-nm Thulium Fiber Laser System

Tm:YAP lasers emitting radiation around 2000-nm have considerable effect in neurosurgery due to it has one of the water absorption peak [16]. It can be coupled into silica fibers which are cheap, easy to use and easily available in the market. However, silica fibers cannot transmit EM radiation when lasers whose wavelengths are grater than 2000-nm are applied [10]. Therefore, thulium fiber lasers are very attractive choice in medical applications especially in minimally invasive surgeries.

In the application of the 1940-nm thulium fiber laser with lamb brain tissues, cortical and subcortical tissues were exposed with a power of 200 mW, 400mW, 600 mW and 800 mW, respectively. Two mode of operation, which are pulsed-modulated mode (pmm) and continuous mode (cm), and also energy densities of 2 J and 4 J were applied to both tissue types. Mean ablation and coagulation diameters and their standart deviations for subcortical and cortical tissues are illustrated in Figure 5.9, Figure 5.10, Figure 5.11 and Figure 5.12. Ablation efficiencies were also showed within the same figures.

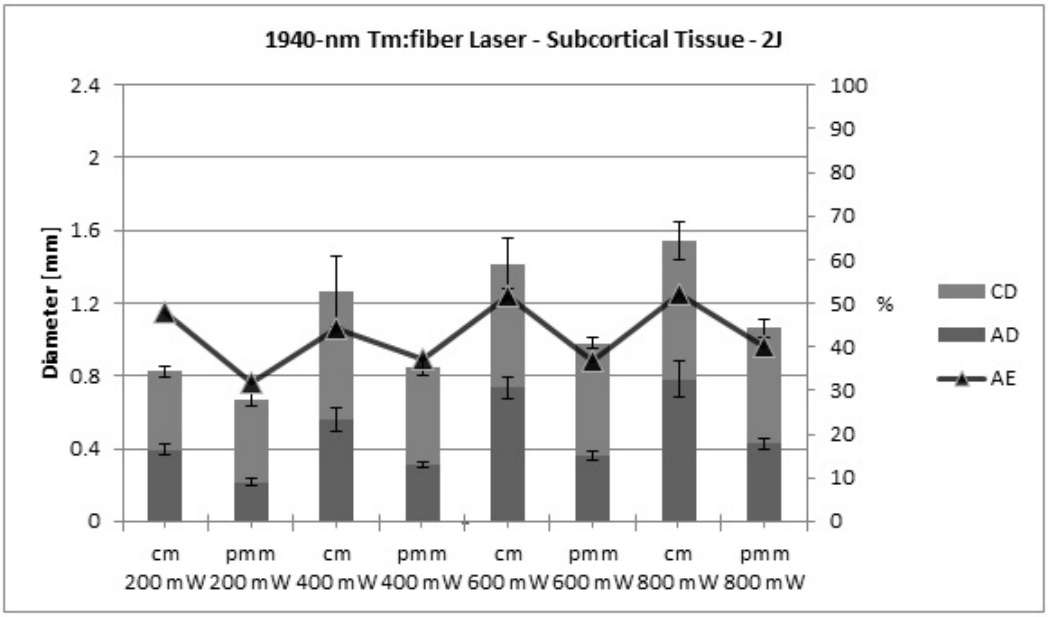

Figure 5.9 The thermal effects and ablation efficiencies of 1940-nm thulium fiber laser on the subcortical tissue at 2 J energy density (CD, coagulated tissue diameter; AD, ablated tissue diameter; AE, ablation efficiency) Y1 axis indicates the diameters of ablated and coagulated tissues, Y2 axis shows the ablation efficiency values, X axis states laser power and mode.

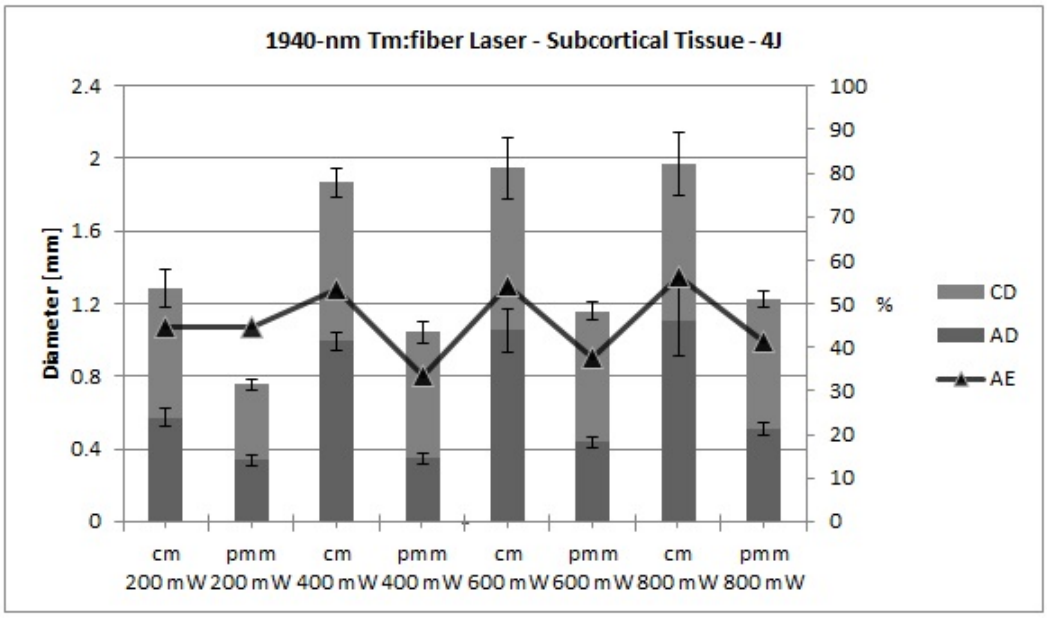

Figure 5.10 The thermal effects and ablation efficiencies of 1940-nm thulium fiber laser on the subcortical tissue at 4 J energy density (CD, coagulated tissue diameter; AD, ablated tissue diameter; AE, ablation efficiency) Y1 axis indicates the diameters of ablated and coagulated tissues, Y2 axis shows the ablation efficiency values, X axis states laser power and mode.

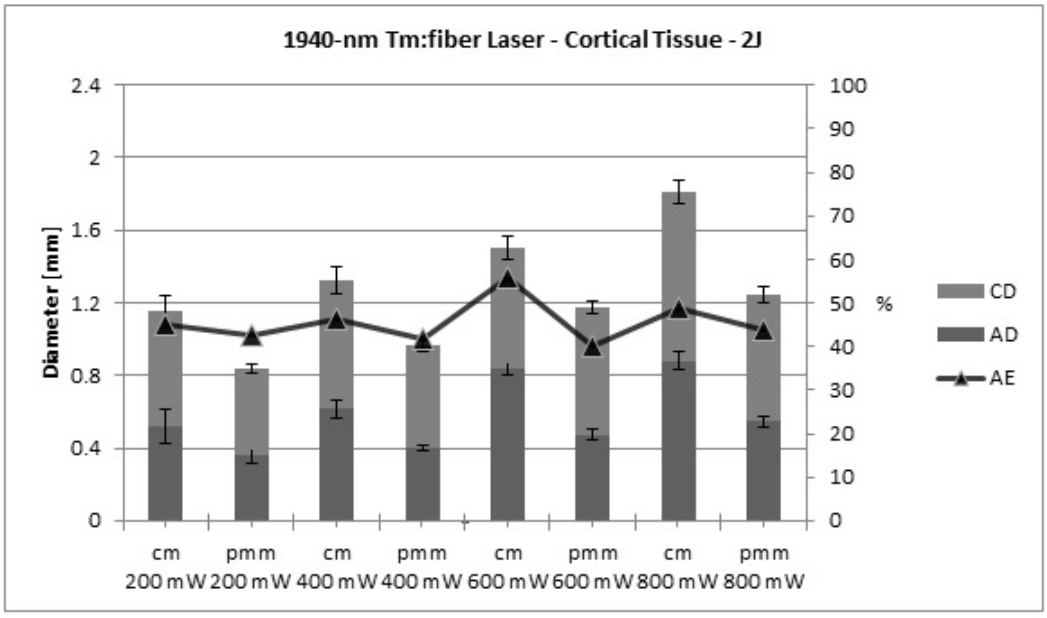

Figure 5.11 The thermal effects and ablation efficiencies of 1940-nm thulium fiber laser on the cortical tissue at 2 J energy density (CD, coagulated tissue diameter; AD, ablated tissue diameter; AE, ablation efficiency) Y1 axis indicates the diameters of ablated and coagulated tissues, Y2 axis shows the ablation efficiency values, X axis states laser power and mode.

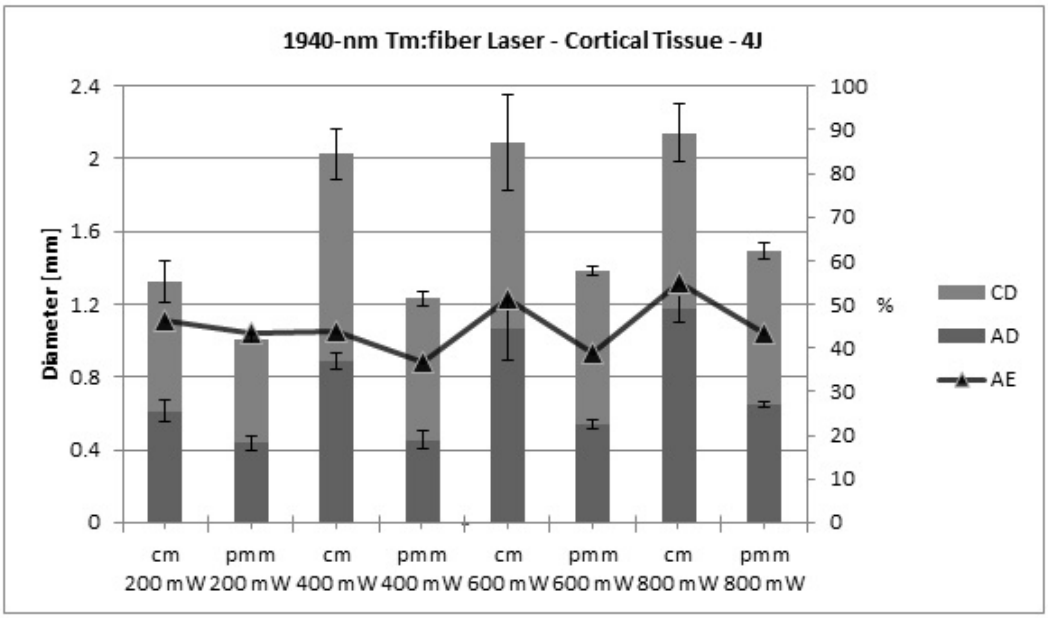

Figure 5.12 The thermal effects and ablation efficiencies of 1940-nm thulium fiber laser on the cortical tissue at 4 J energy density (CD, coagulated tissue diameter; AD, ablated tissue diameter; AE, ablation efficiency) Y1 axis indicates the diameters of ablated and coagulated tissues, Y2 axis shows the ablation efficiency values, X axis states laser power and mode.

When power levels are compared statistically, it was found that there is no significant differences between 0.6 mW and 0.8 mW power levels for cm applications, both tissue types and both energy densities ($P<0.2$). However, there is significant differences for other cm applications and all pmm application in terms of power levels ($P<0.001$). Besides, variations of mode of operations ($P<0.001$), energy denisities ($P<0.001$)and tissue types ($P<0.001$) have significant differences.

As the power is increased, diameters of coagulation and ablation increase in nearly all types of application ($P<0.001$). It was found that there is remarkable differences between the modes (cm and pmm) for the same energy and power ($P<0.001$). Continuous mode investigations show more ablation and photothermal effect on the not only cortical tissue but also subcortical tissue ($P<0.001$). Besides, ablation efficiencies are higher in the cm applications when compared to the pmm applications ($P<0.001$). Diameter values of cortical tissue are significantly higher then the subcortical tissue in both energy densities ($P<0.001$). Eventually, it was found that the highest ablation efficiencies are 56.01 percent and 54.83 percent for subcortical and cortical tissues in

the power of 0.8 W, energy density of 4 J and cm applications, respectively.

5.3.2 1470-nm Diode Laser System

The second dosimetry study was done with 1470-nm diode laser. In this investigation, energy density of 2 J and 4 J with cm and pmm operations as 1940-nm thulium fiber laser application were used, and also both lamb brain tissues were exposed with the power of 0.5 W, 1 W, 1.5 W and 2 W, respectively. Obtained experiment results are showed in Figure 5.13, Figure 5.14, Figure 5.15 and Figure 5.16. Figure 5.13 and Figure 5.14 give the mean ablation and coagulation diameters with their standart deviations for subcortical tissue with the energy densities of 2 J and 4 J. Figure 5.15 and Figure 5.16 illustrate same parameters for cortical tissue like previous two graphs. Besides, ablation efficiencies were added withing the same graphs.

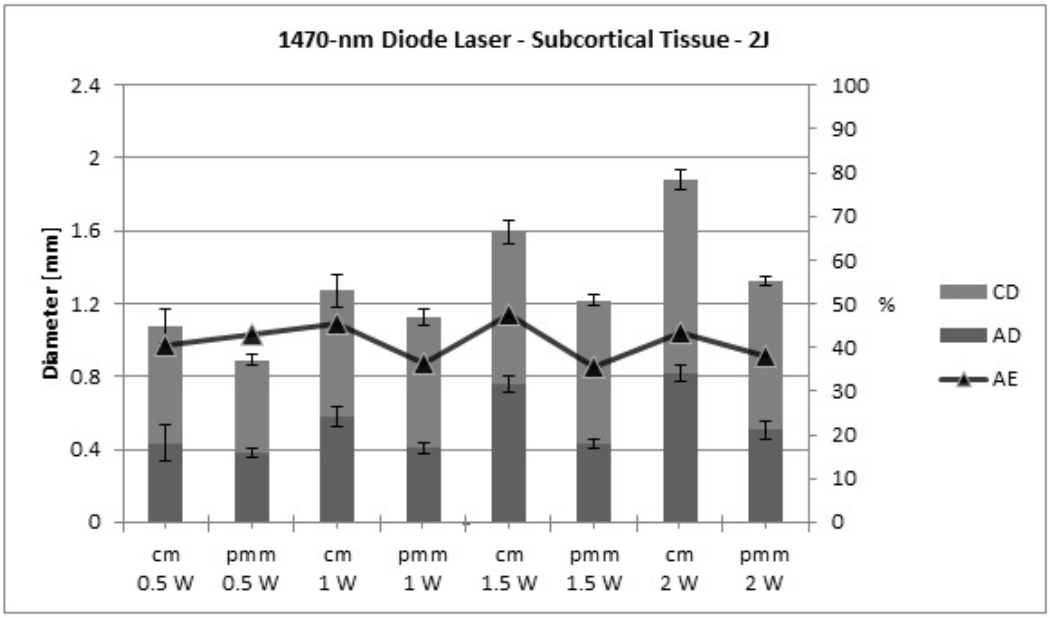

Figure 5.13 The thermal effects and ablation efficiencies of 1470-nm diode laser on the subcortical tissue at 2 J energy density (CD, coagulated tissue diameter; AD, ablated tissue diameter; AE, ablation efficiency) Y1 axis indicates the diameters of ablated and coagulated tissues, Y2 axis shows the ablation efficiency values, X axis states laser power and mode.

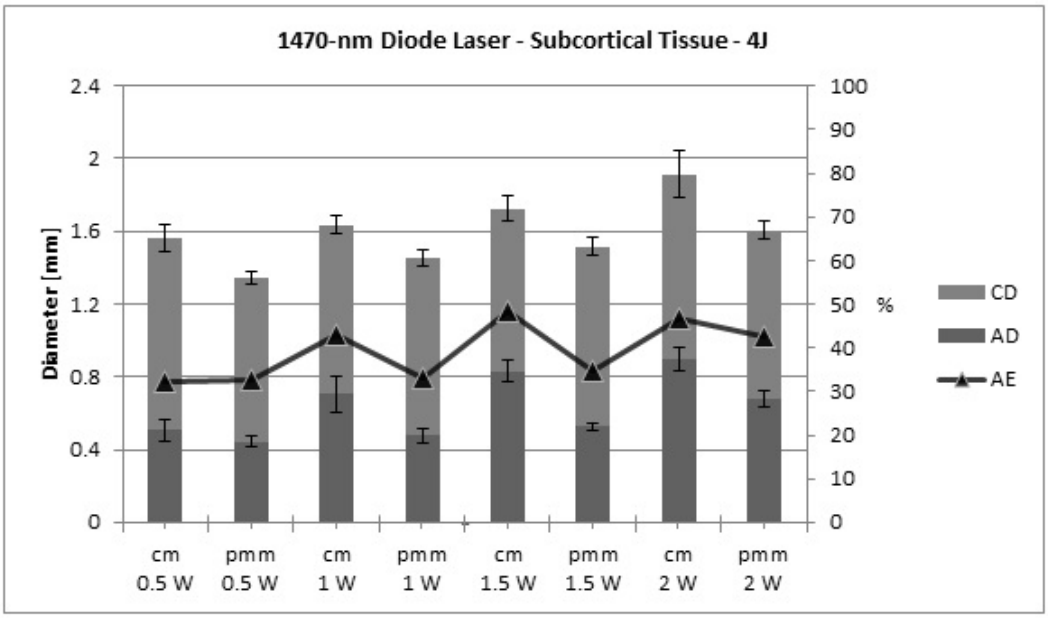

Figure 5.14 The thermal effects and ablation efficiencies of 1470-nm diode laser on the subcortical tissue at 4 J energy density (CD, coagulated tissue diameter; AD, ablated tissue diameter; AE, ablation efficiency) Y1 axis indicates the diameters of ablated and coagulated tissues, Y2 axis shows the ablation efficiency values, X axis states laser power and mode.

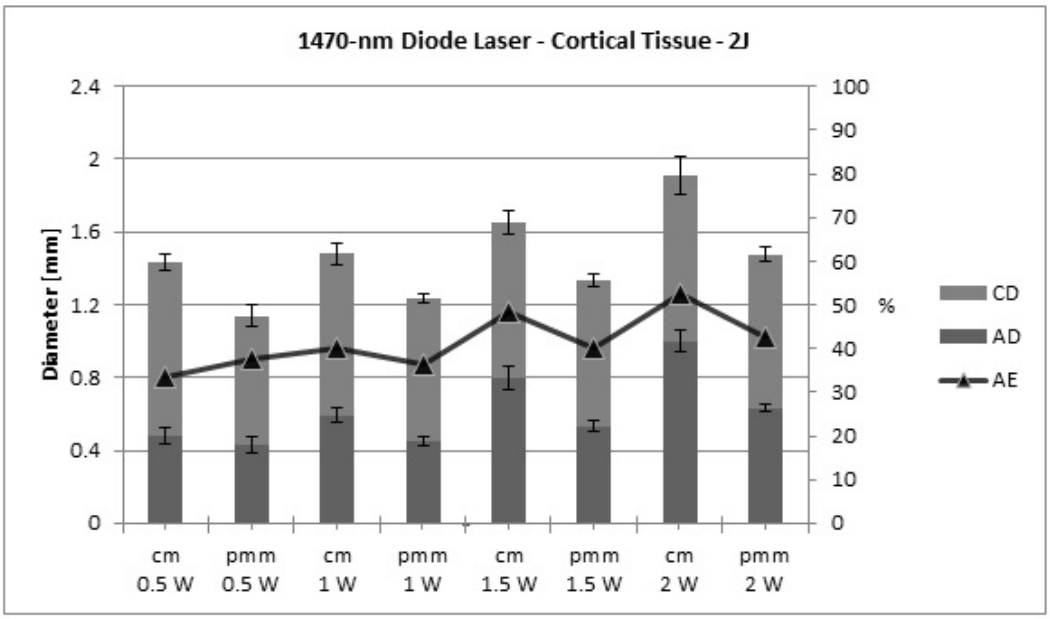

Figure 5.15 The thermal effects and ablation efficiencies of 1470-nm diode laser on the cortical tissue at 2 J energy density (CD, coagulated tissue diameter; AD, ablated tissue diameter; AE, ablation efficiency) Y1 axis indicates the diameters of ablated and coagulated tissues, Y2 axis shows the ablation efficiency values, X axis states laser power and mode.

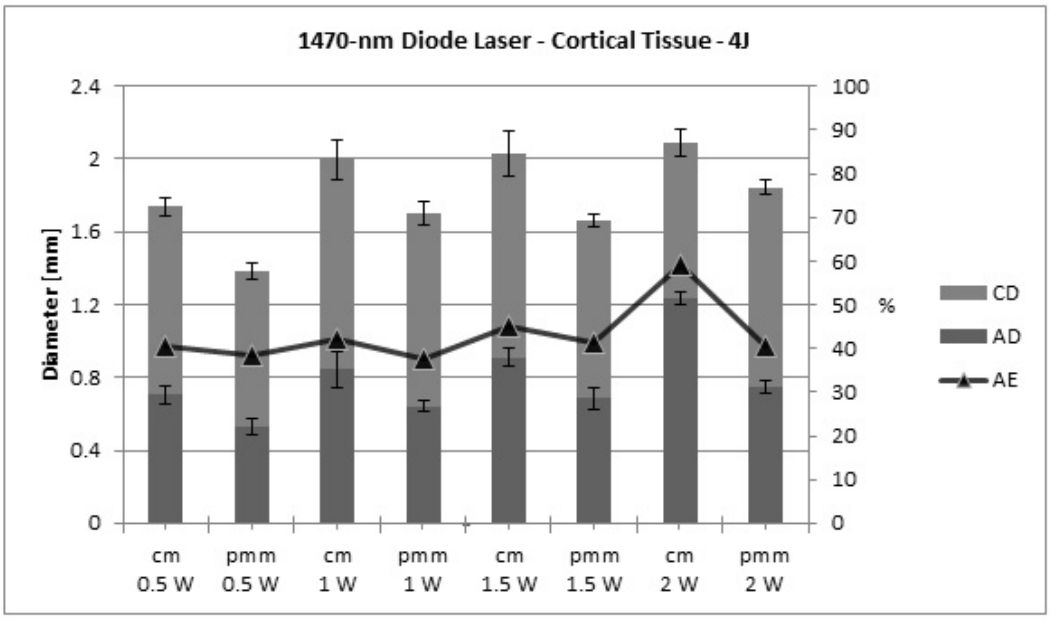

Figure 5.16 The thermal effects and ablation efficiencies of 1470-nm diode laser on the cortical tissue at 4 J energy density (CD, coagulated tissue diameter; AD, ablated tissue diameter; AE, ablation efficiency) Y1 axis indicates the diameters of ablated and coagulated tissues, Y2 axis shows the ablation efficiency values, X axis states laser power and mode.

It was found that when the diameters of coagulated and ablated tissues were compared statistically, each of the laser output powers ($P<0.001$), energy densities ($P<0.001$), tissue types ($P<0.001$) and mode of operations ($P<0.001$) has significant differences. However, laser output power has an exception for ablation diameters when the subcortical tissue is exposed with pmm at 2 J ($P<0.3$). In this investigation, when compared the Tm:fiber laser application and this application, similar results were found. For instance, diameters of the ablation and thermally altered areas increase as the power is increased, and cm applications show higher ablation efficiency, ablation and photothermal effect ($P<0.001$). These cases are valid for both tissue types. Ultimately, cm 1.5 W with 4 J energy density generates 48.25 percent ablation efficiency for the subcortical tissue while cm 2 W with 4 J energy density produces 59.21 percent ablation efficiency for the cortical tissue. These values are the highest ablation efficiencies.

5.3.3 1070-nm Ytterbium Fiber Laser System

Nd:YLF laser whose wavelength is 1070-nm has the lower absorption coefficient among four lasers. Therefore, the laser beam scatters inside of the tissue, and temperature of the tissue cannot suddenly reach to 100 °C. This leads to no absorption effect but coagulation effect on the both tissues. Obtained experimental results are illustrated in Figure 5.17, Figure 5.18, Figure 5.19 and Figure 5.20. Figure 5.17 and Figure 5.18 show the coagulation diameters for the subcortical tissue for with 20 J and 40 J energy densities while the other last figures illustrate the coagulation diameters for cortical tissue with same energy densities. Ablation efficiency cannot be calculated because there is no absorption effect on the tissue. In this investigation, it was found that responses of the both tissue types are different statistically for each parameters ($P<0.001$). Besides, the power or energy density is increased, the diameter of the photo-thermal effect increase ($P<0.001$).

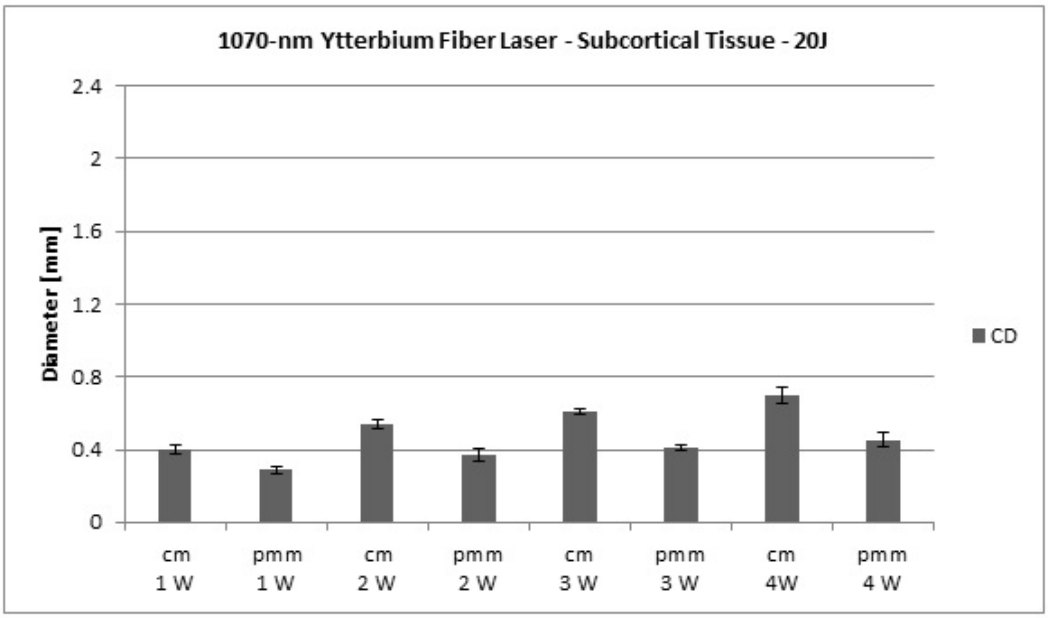

Figure 5.17 The thermal effect of 1070-nm ytterbium fiber laser on the subcortical tissue at 20 J energy density (CD, coagulated tissue diameter) Y axis shows the diameters of coagulation, X axis indicates laser power and mode.

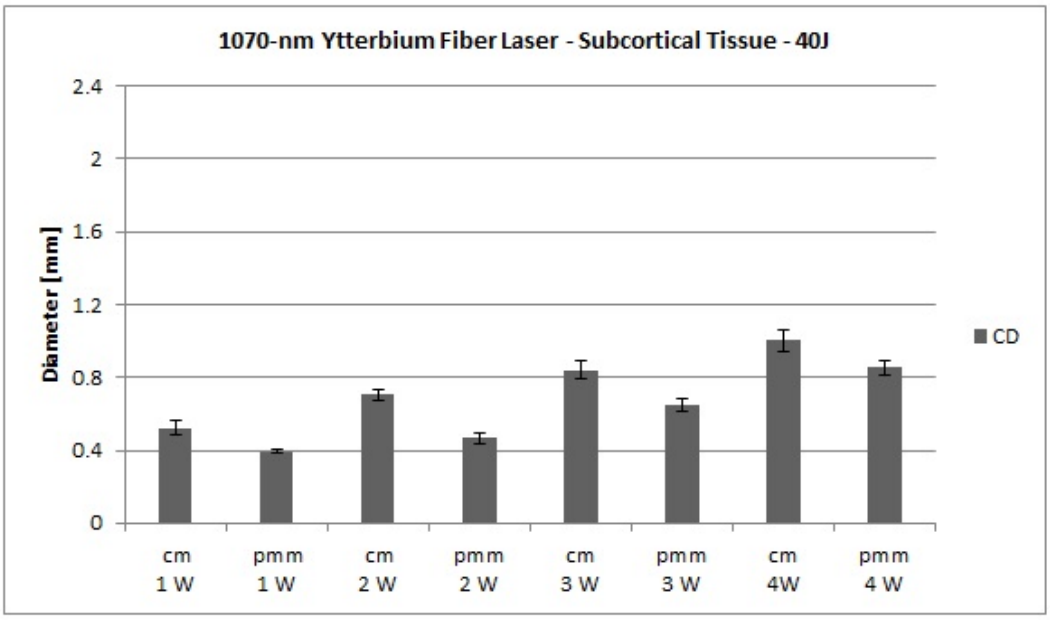

Figure 5.18 The thermal effect of 1070-nm ytterbium fiber laser on the subcortical tissue at 40 J energy density (CD, coagulated tissue diameter) Y axis shows the diameters of coagulation, X axis indicates laser power and mode.

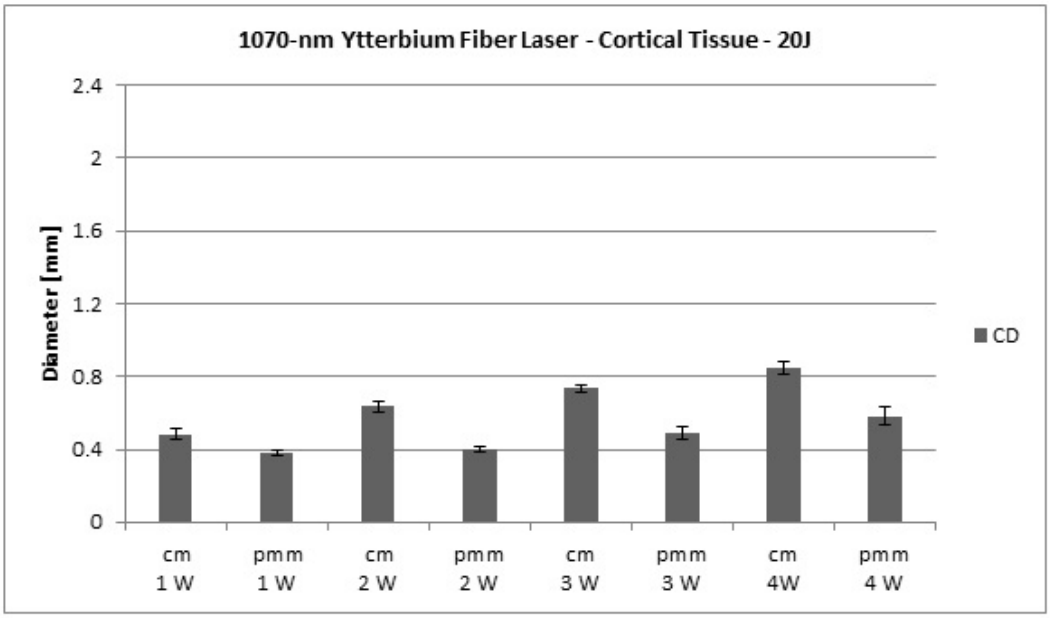

Figure 5.19 The thermal effect of 1070-nm ytterbium fiber laser on the cortical tissue at 20 J energy density (CD, coagulated tissue diameter) Y axis shows the diameters of coagulation, X axis indicates laser power and mode.

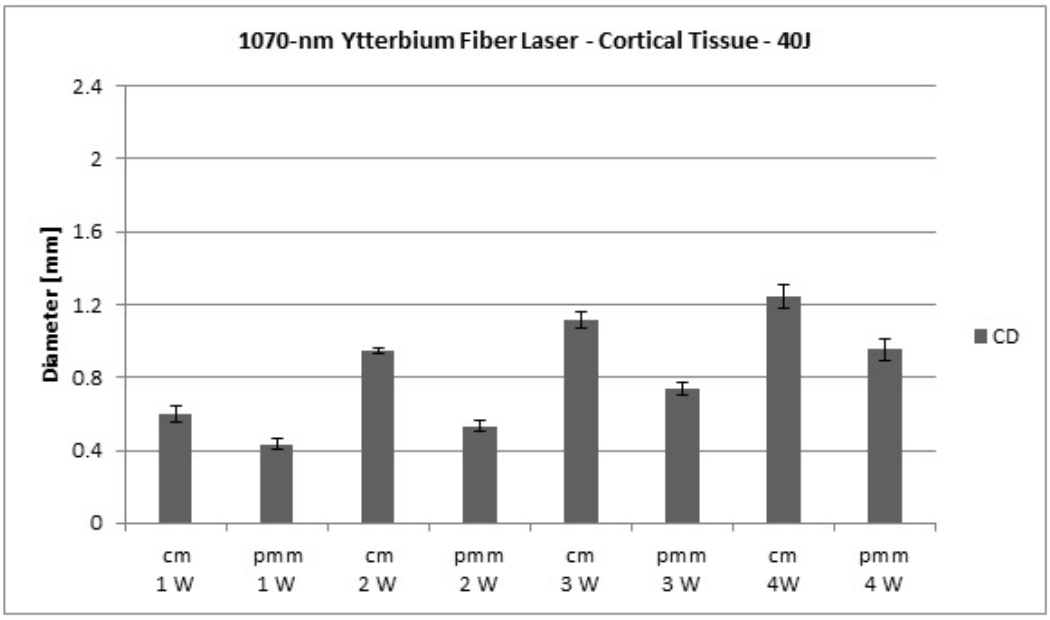

Figure 5.20 The thermal effect of 1070-nm ytterbium fiber laser on the cortical tissue at 40 J energy density (CD, coagulated tissue diameter) Y axis shows the diameters of coagulation, X axis indicates laser power and mode.

5.3.4 980-nm Diode Laser System

980-nm diode laser has one of the absorption coefficient peak in the near infrared spectrum that gives it more coagulation diameters than the previous study. In other words, laser beam of the 980-nm diode laser penetrates more when comparing the laser beam of 1070-nm ytterbium laser. In this investigation, ablation diameter was not observed under the microscope at least energy densities of 20 J and 40 J. The results of this laser application for cortical as well as subcortical tissues are illustrated in Figure 5.21, Figure 5.22, Figure 5.23 and Figure 5.24. It was statistically found that diameters of the both tissue effects vary with the vaiations of all parameters ($P<0.001$). In other words, thermally altered areas are higher than the previous experiment, and cm applications generate more thermally altered zone than the pmm applications ($P<0.001$). Eventually, cortical tissue has greater coagulated lesions than the subcortical tissue ($P<0.001$).

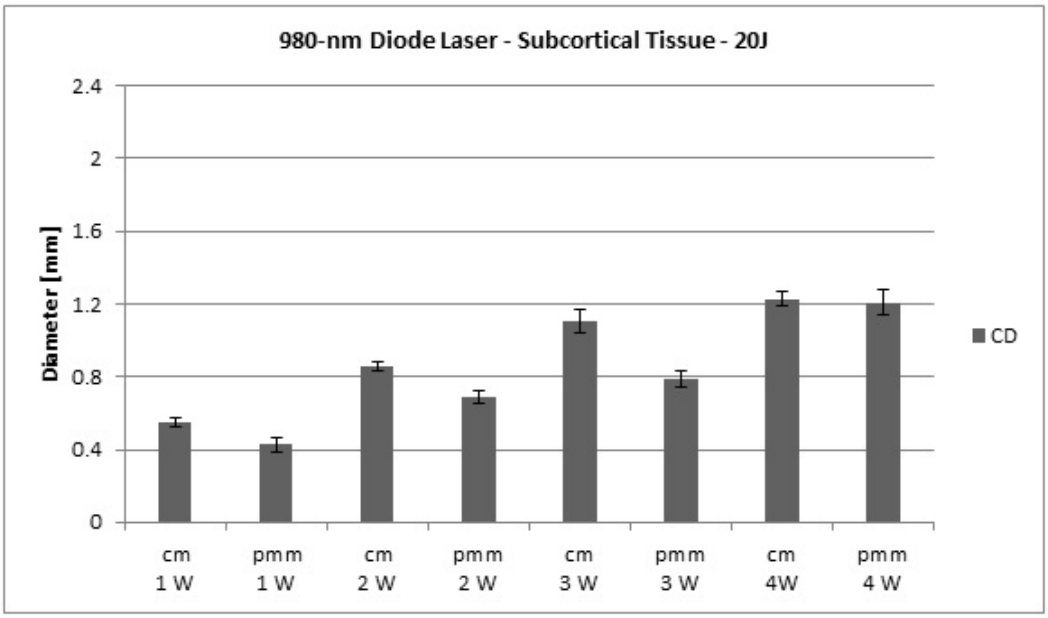

Figure 5.21 The thermal effect of 980-nm diode laser on the subcortical tissue at 20 J energy density (CD, coagulated tissue diameter) Y axis shows the diameters of coagulation, X axis indicates laser power and mode.

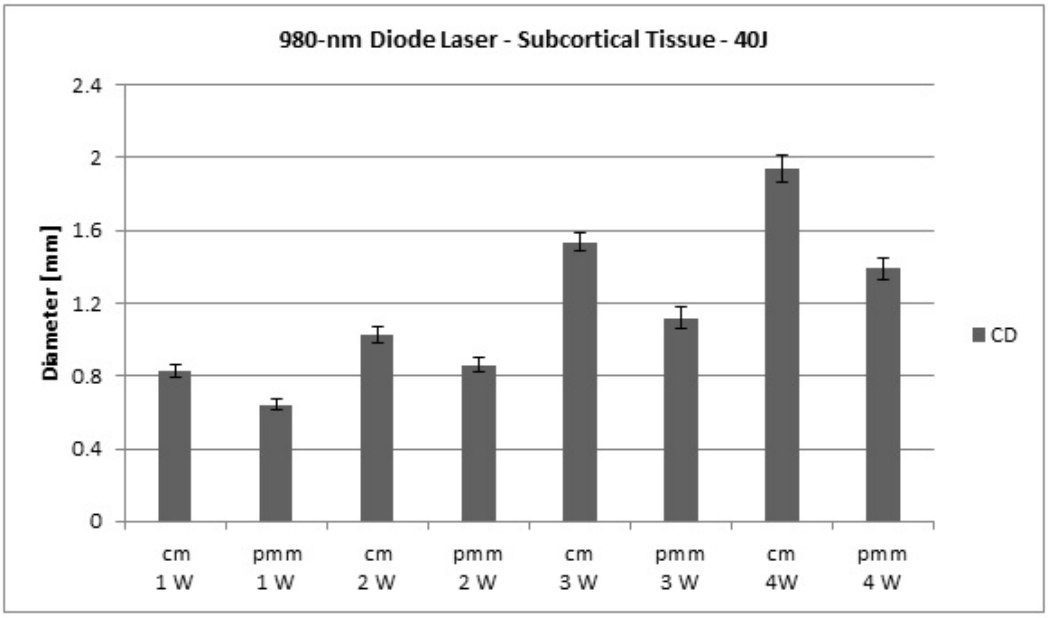

Figure 5.22 The thermal effect of 980-nm diode laser on the subcortical tissue at 40 J energy density (CD, coagulated tissue diameter) Y axis shows the diameters of coagulation, X axis indicates laser power and mode.

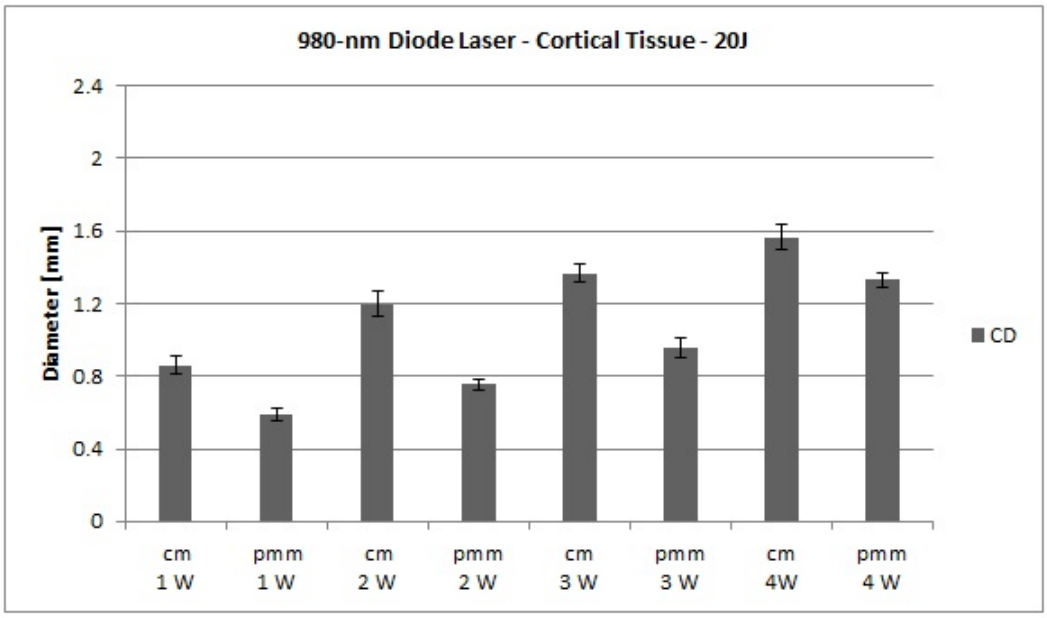

Figure 5.23 The thermal effect of 980-nm diode laser on the cortical tissue at 20 J energy density (CD, coagulated tissue diameter) Y axis shows the diameters of coagulation, X axis indicates laser power and mode.

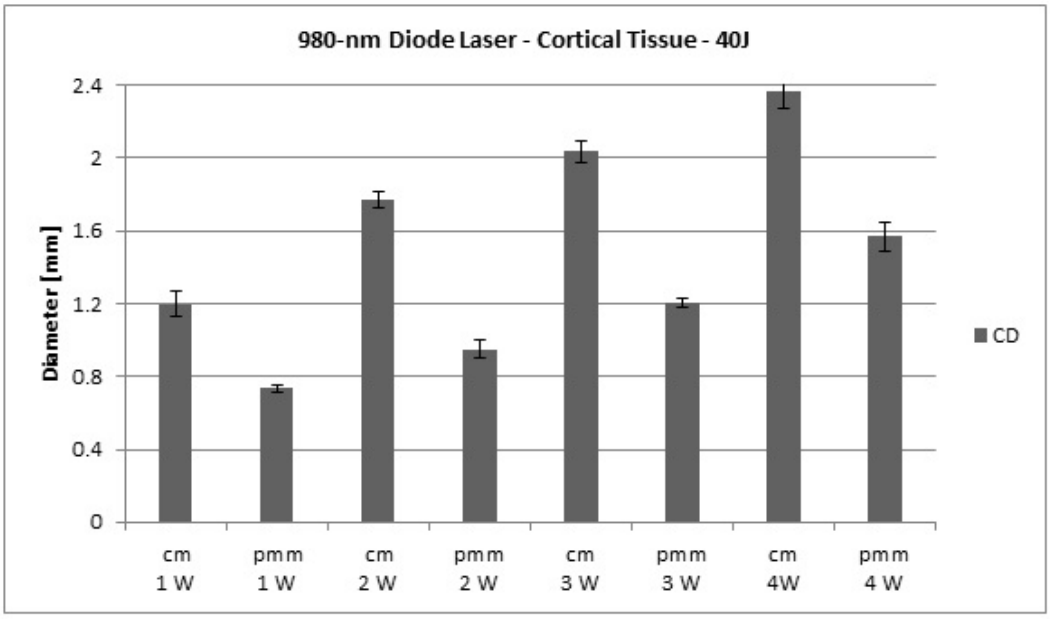

Figure 5.24 The thermal effect of 980-nm diode laser on the cortical tissue at 40 J energy density (CD, coagulated tissue diameter) Y axis shows the diameters of coagulation, X axis indicates laser power and mode.

5.4 Discussion

Scientists have been investigating laser-brain-ablation over 3 decades in spite of the fact that this method is not widely used in the clinic. Main factor is that relationship between parameters and laser-tissue interaction mechanism is not known very well. These parameters are tissue parameters (such as thermal conductivity, tissue density and absorptivity), laser parameters (like laser type, exposure time, wavelength, energy density, power, operation mode, pulse duration and pulse repetition) and environmental parameters (such as environmental medium and its temperature) [28]. These parameters are related to conduction of heat that when laser beam contacts with the tissue itself, transformation the radiation energy to heat occurs. This leads to tissue temperature raise, and causes to denaturation of protein, dehydration, carbonization, coagulation and ablation [29]. Variations of the optical features with temperature change mechanism of the laser irradiation and the tissue response [30, 31]. For instance, when the tissue is exposed to continuous laser radiation, temperature of the tissue continuously increases that leads to a change in absorption coefficient because dehydrate occurs with temperature rise, and water content in the tissue changes [32, 33]. Besides, local inhomogeneities and individual differences in the tissue make difficult the best dose estimation. In other words, dynamic changes with respect to the inhomogeneities of the tissue cause a catastrophic carbonization and melting when laser is irradiated [34].

In order to propose an appropriate laser as a surgical tool for the neurosurgery, a well defined dosimetry study to find a safe operating region is necessity. Therefore, ablation efficiency was defined by our group [35], and it gives an idea about the efficiency of the dose in the way of thermally removed tissue with the irreversible thermal damage. The diameters of coagulation and ablation areas were measured by using a light microscope. To provide less thermal effect to the nearby healthy tissue is the most essential factor in the surgical operations. Moreover, the main problem is that some lasers do not remove brain tumors but only coagulate them. In this way, necrotic tissue remains inside the brain and leads to the occurrence edema [4]. In other words, coagulated tissue is unwanted in neurosurgical applications; therefore, ablation efficiency

guides the success of laser brain ablation treatment. It can be said that when the coagulated area gets close to the ablated area, value of the ablation efficiency increase, and the best dosimetry for the brain ablation can be relatively obtained. However, inhomogeneities and dynamic changes of the tissue get harder to find appropriate laser parameters.

Many scientists determined many parameters in different applications, but they did not investigate several lasers for brain ablation in one paper. Thus, it is hard to comment these researchers findings comparatively. In this study, brain ablation efficiencies are compared by using four infrared laser devices which are 1940-nm thulium fiber laser, 1470-nm diode laser, 1070-nm ytterbium fiber laser, and 980-nm diode laser. In this way, most appropriate laser could be proposed for clinical use.

The absorption coefficient of water is essential parameter in medical laser applications and causes different wavelengths to penetrate different distances into the tissues. Therefore, different lasers effect the tissue removal differently. Besides, higher absorption coefficient of water leads to less penetration depth, causes to precise tissue ablation and less tissue damage. It should not be forgotten that during the laser radiation, the water content in the tissue changes dynamically that leads to dynamic absorption coefficient [32, 33].

These four laser devices which were used in the investigation can be connected with the silica fibers effectively. Silica fibers are easy-to-use, cheap and suitable for minimally invasive surgery (MIS) [10]. MIS, which is a surgical technique, allows patients to recover faster and heal with less scarring and pain.

Tm:fiber laser whose wavelength is 1980-nm, has the highest absorption coefficient of water among other lasers which were used in the investigation. Moreover, this laser is almost only laser which can be coupled with a silica fiber because silica fibers cannot carry radiation of wavelengths greater than 2000-nm [10]. Thus, 1980-nm Tm:fiber laser is very attractive choice in neurosurgery. Tm:fiber lasers have remarkable potential for neurosurgery by overlapping one of the peak absorption co-

efficient of the water [16, 35]. 2000-nm laser applications were widely investigated. For example, Nishioka et al. investigated 2120-nm pulsed-holmium laser and 2010-nm pulsed-thulium laser in terms of their ablation rates in a vitro study. They found that thulium laser has better effects than the other one that latter laser provides less thermal effect to the nearby healthy tissue [16]. However, there is not enough study with 1940-nm thulium fiber laser in the literature.

In the near infrared spectrum (800-1200 nm), laser radiations are poorly absorbed by water compared to the infrared lasers[36]. 980-nm is an exception in the near infrared spectrum that it has one of the absorption coefficient peak, and 980-nm diode laser was reported a successful surgical tool [14, 15]. Besides, 1070-nm ytterbium fiber laser which was used in the experiment is situated in the near infrared spectrum with low absorption coefficient. These lasers are in tendency to scatter inside the tissue and gives huge damage to the neural tissue [8]. In spite of the poor absorption by water in the near infrared region, hemoglobine absorption is relatively high and these lasers have advantage of coagulating blood vessels [11].

1470-nm diode laser has the second highest absorption coefficient among four lasers which were used in the experiments. Ulrich et al. used a Nd:YAG laser whose wavelength is 1319-nm with a 200μm silica fiber. They found that 1319-nm Nd:YAG laser can be suitable for neurosurgery because it gave appropriate ablation and coagulation results. Characteristics of 1470-nm diode laser such as absorption coefficient is almost same with Nd:YAG laser because of the fact that wavelengths of the 1470-nm diode and Nd:YAG lasers are almost same. For this reason, it was found in this investigation that 1470-nm diode laser is successful for brain ablation like Nd:YAG laser.

In this investigation, four lasers were applied to both cortical and subcortical tissues. Because of their different absorption coefficients with water, interaction of each laser beam is different; therefore, different ablation and coagulation diameters, and also ablation efficiencies were obtained. It was found that ablation and coagulation diameters can be changed by laser power ($P<0.001$), energy density ($P<0.001$), mode of

operation ($P<0.001$) and tissue type ($P<0.001$). 1980-nm thulium fiber laser and 1470-nm diode laser beams generate ablated tissues in both cortical and subcortical lamb brain tissues. However, the other lasers which are 1070-nm ytterbium fiber laser and 980-nm diode laser cannot remove lamb brain tissue although they delivered ten times bigger amount of energy than the first two lasers. Namely, 1940-nm Tm:fiber laser and 1470-nm diode laser delivered 2 J and 4 J while 1470-nm ytterbium fiber laser and 980-nm diode laser used 20 J and 40 J energy densities. This can be explained that 1980-nm thulium fiber laser and 1470-nm diode laser have the highest absorption coefficients of water in comparison with the other two lasers. Moreover, ablation efficiency was calculated for only 1940-nm Tm:fiber laser and 1470-nm diode laser. Although these ablation efficiency values are given in the dosimetry study section diagrammatically, these values are summarized in Table 5.1 and Table 5.2.

Table 5.1
Ablation efficiencies of 1940-nm thulium fiber laser.

	Ablation Efficiency in Subcortical Tissue [%]		**Ablation Efficiency in Cortical Tissue [%]**	
Power	**2 [J]**	**4 [J]**	**2 [J]**	**4 [J]**
cm 0.2W	47.87	44.47	44.87	46.26
pmm 0.2 W	31.9	44.77	42.38	43.39
cm 0.4 W	44.36	53.30	46.45	43.81
pmm 0.4 W	37.19	33.60	41.90	36.82
cm 0.6 W	51.83	53.97	55.76	51.20
pmm 0.6 W	36.69	37.57	40.27	38.81
cm 0.8 W	52.00	**56.01**	48.67	54.83
pmm 0.8 W	40.07	41.23	43.84	43.34

It is obvious that the highest ablation efficiency for the subcortical tissue can be obtained when 1940-nm thulium fiber laser with combination of 800 mW power output, 4 J energy density and continuous operation mode is used. Besides, 1470-nm diode laser can be used for cortical brain ablation with 2 W power output, 4 J energy density

Table 5.2
Ablation efficiencies of 1470-nm diode laser.

	Ablation Efficiency in Subcortical Tissue [%]		**Ablation Efficiency in Cortical Tissue [%]**	
Power	**2 [J]**	**4 [J]**	**2 [J]**	**4 [J]**
cm 0.5W	40.49	32.39	33.44	40.55
pmm 0.5 W	42.92	32.76	37.74	38.40
cm 1 W	45.61	43.17	40.12	42.16
pmm 1W	36.18	32.89	36.43	37.77
cm 1.5 W	47.60	48.25	48.48	44.84
pmm 1.5 W	35.43	34.74	39.94	41.26
cm 2 W	43.42	46.8	52.44	**59.21**
pmm 2W	38.11	42.44	42.76	40.56

and continuous mode operation. In other words, 1980-nm Tm:fiber laser and 1470-nm diode laser should be used together for brain ablation. 1070-nm ytterbium fiber laser and 980-nm diode laser did not generate any ablated area on not only cortical tissue but also subcortical tissue at least 20 J and 40 J energy densities. Therefore, they are not appropriate lasers for brain ablation but they can be used as a coagulator. Moreover, 980-nm diode laser has greater coagulation diameters on both tissue types than 1070-nm ytterbium fiber laser has. This can be explained that 980-nm diode laser has one of the peak absorption coefficient of water. Therefore, it has less scattering effect on the tissue.

In the investigation, same amount of energy density was used by 1980-nm Tm:fiber laser and 1470-nm diode laser. It was found that pmm laser applications have lower ablation efficiencies when compared to cm laser applications ($P<0.001$). This situation is valid for both lasers, and can be explained that tissue cools itself down, and transmit the heat to surrounding tissue in the pmm applications. In this way, temperature raise in the tissue is minimum, which causes higher coagulation diameters and lower ablation diameters, and also smaller ablation efficiencies [34]. More-

over, the ablation efficiencies and diameters of coagulation and ablation are different in both tissues because their optical features are different [5]. Diameters of coagulation and ablation areas are higher for the cortical tissue ($P<0.001$). Subcortical tissue has higher myelin sheaths which consist of lipids; therefore, water absorption coefficient of subcortical tissue is low, which leads to smaller coagulation and ablation diameters [34].

Consequently, it is aimed to compare interaction mechanisms of four different lasers with lamb brain tissue in this investigation. In the literature, there is not adequate number of papers which compare several lasers in only one paper for brain ablation. For this reason, it is hard to comment these scientists findings. In order to suggest appropriate parameters (such as wavelength, mode of operation, duration of exposure and energy density) for clinical use, pre-dosimetry and dosimetry studies were done. 1940-nm thulium fiber laser and 1470-nm diode laser can remove brain tissues, and it was found that 1940-nm thulium fiber laser can be used for subcortical tissue while 1470-nm diode laser is useful in cortical ablation.

6. CONCLUSION AND FUTURE WORKS

In this investigation, four infrared lasers were used in order to find appropriate laser for neurosurgery. These lasers are 1940-nm thulium fiber laser, 1470-nm diode laser, 1070-nm ytterbium fiber laser and 980-nm diode laser. Before dosimetry study, pre-dosimetry study was conducted for each laser. In this way, coagulation and carbonization onset times were obtained for cortical and subcortical tissues, and safe operation area was defined for dosimetry study. In the pre-dosimetry study, some lasers did not show any carbonization at least in 240 seconds up to some power outputs. However, carbonization and coagulation onset times decrease when the output power is increased. After the pre-dosimetry study, dosimetry study was carried out that two level of the energy densities were applied to both tissue types. 2 J and 4 J energy densities were applied in 1940-nm thulium fiber laser and 1470-nm diode laser applications while 20 J and 40 J energy density applications were done with 1070-nm ytterbium fiber laser and 980-nm diode laser. Moreover, not only cm but also pmm were used in all laser applications with 4 different power levels. In 1940-nm thulium fiber laser application, laser power outputs of 200 mW to 800 mW with 200 mW increments were used. On the other hand, in 1470-nm diode laser application, laser power outputs of 0.5 W to 2 W with 0.5 W increments were applied. Eventually, 1070-nm ytterbium fiber laser and 980-nm diode laser applications used power of 1-4 W with 1 W increment. Besides, 100-ms on and 100-ms off cycle of wave was used in pmm applications.

Cortical tissue has greater ablation and coagulation diameters due to the fact that subcortical tissue has higher myelin sheaths which causes lower water absorption coefficient and coagulation-ablation diameter. Moreover, pulsed-modulated laser irradiation leads to cool tissue down, greater diameter of coagulation and smaller diameter of ablation. Therefore, ablation efficiencies of the pulsed-modulated applications are lower than the ablation efficiencies of the continuous-mode laser applications [37]. It is found that 1940-nm thulium fiber laser and 1470-nm diode laser can be used as a

brain ablator for subcortical and cortical tissues, respectively.

When a laser radiates to the tissue, tissue temperature raises which results with ablation of the tissue by vaporizing it. So as to obtain more precise brain ablation and less thermal effect to the nearby tissue, the tissue temperature should be monitored during laser application. Temperature alters during laser operation could be good indicator to predict and understand the tissue response to the laser beam. Moreover, it is known that in vivo conditions, blood circulation behave as a coolant. Therefore, temperature changes should be monitored during the operation, and also histological tests should be conducted on animals [34].

REFERENCES

1. Choy, D. S., "History of lasers in medicine," *The Thoracic and Cardiovascular Surgeon*, Vol. 36, no. 2, pp. 114–117, 1988.

2. Liao, H., and K. Fujiwara, "Automatic laser scanning ablation system for high-precision treatment of brain tumors," *Springer*, Vol. 28, pp. 891–900, May 2013.

3. Avgeropulus, N. G., and T. T. Batchelor, "New treatment strategies for malignant gliomas," *Oncologist*, Vol. 4, pp. 209–224, 1999.

4. Niemz, M. H., *Laser tissue interactions fundamentals and applications*, Heidelberg: Springer, 3rd ed., 2003.

5. Fillerup, D. L., and J. F. Mead, "The lipids of the aging human brain," *Lipids*, Vol. 2, pp. 295–298, 1967.

6. Prasad, P. N., *Introduction to biophotonics*, USA: Wiley Interscience, 2003.

7. Çilesiz, I., and S. Thomsen, "Controlled temperature tissue fusion: Ho:yag laser welding of rat intestine in vivo, part two," *Lasers in Surgery and Medicine*, Vol. 21, pp. 278–286, 1997.

8. Downing, E. F., and et al., *Lasers in neurosurgery*, Springer, 1989.

9. Devaux, B. C., and et al., "High-power diode laser in neurosurgery: clinical experience in 30 cases," *Surgical Neurology*, Vol. 50, no. 1, pp. 33–40, 1998.

10. El-Sherif, A. F., and T. A. King., "Soft and hard tissue ablation with short-pulse high peak power and continuous thulium-silica fiber lasers," *Lasers in Medical Science*, Vol. 18, pp. 139–147, 2003.

11. Peavy, G. M., "Lasers and laser-tissue interaction," *The Veterinary Clinics Small Animal Practice*, Vol. 32, no. 3, pp. 517–534, 2002.

12. Gulsoy, M., and et al., "Er:YAG laser ablation on cerebellar and cerebral tissue," *Lasers in Medical Science*, Vol. 16, pp. 40–43, 2001.

13. Boggan, J. E., and M. S. B. Edwards, "Comparison of the brain tissue response in rats to injury by argon and carbon dioxide lasers," *Neurosurgery*, Vol. 11, no. 609–616, 1982.

14. O Bozkulak, e. a., "The 980 nm diode laser for brain surgery: histopathology and recovery period," *Lasers in Medical Science*, Vol. 19, pp. 41–47, 2004.

15. Gulsoy, M., and et al., "Application of the 980 nm diode laser in stereotaxic surgery," *IEEE J. Sel. Top. Quantum Electron*, Vol. 5, no. 2, pp. 1090–1094, 1999.

16. Nishioka, N. S., and Y. Domankevitz, "Comparison of tissue ablation with pulsed holmium and thulium lasers," *IEEE J. of Quantum Electron*, 1990.

17. Simhon, D., and et al., "Laser soldering of rat skin, using fiber-optic temperature controlled system," *Lasers in Surgery and Medicine*, Vol. 29, pp. 265–273, 2001.

18. Simhon, D., and et al., "Closure of skin incisions in rabbits by laser soldering: I: wound healing pattern," *Lasers in Surgery and Medicine*, Vol. 35, pp. 1–11, 2004.

19. Brosh, T., and et al., "Closure of skin incisions in rabbits by laser soldering: Ii: tensile strength," *Lasers in Surgery and Medicine*, Vol. 35, pp. 12–17, 2004.

20. Forer, B., and et al., "Repair of pig dure in vivo using temperature controlled co laser soldering," *Lasers in Surgery and Medicine*, Vol. 37, no. 4, pp. 286–292, 2005.

21. Bozkulak, O., "Comparison of 980 nm diode laser and electrolytic lesions in rat brain by SDS-PAGE and CD68," Master's thesis, Bogazici University, Istanbul, Turkey, 2003.

22. Bartels, K. E., "Lasers in medicine and surgery," *The Veterinary Clinics Small Animal Practice*, Vol. 32, no. 3, pp. 495–515, 2002.

23. Robertson, J. H., and W. C. Clark, *Lasers in Neurosurgery*, USA: Kluwer Academic Publishers, 1988.

24. Sullins, K. E., "Diode laser and endoscopic laser surgery," *The Veterinary Clinics Small Animal Practice*, Vol. 32, no. 3, pp. 639–648, 1999.

25. Gulsoy, M., *Laser systems for biomedicine: Introduction the 980 nm diode laser.* PhD thesis, Istanbul Technical University, Istanbul, Turkey, 2000.

26. Korkmaz, Y., "Investigation of 980 nm diode laser parameters for sogt tissue surgery," Master's thesis, Bogazici University, Istanbul, Turkey, 2006.

27. Merigo, E., and et al., "Laser-assisted surgery with different wavelengths: preliminary ex vivo study on thermal increase and histological evaluation," *Lasers in Medical Science*, Vol. 28, no. 2, pp. 497–504, 2013.

28. McKenzie, A. L., "Physics of thermal process in laser-tissue interaction," *Physics in Medicine and Biology*, Vol. 35, pp. 1175–1209, 1990.

29. Welch, A. J., and M. J. C. Gemert, *Optical - thermal response of laser-irradiated tissue*, New York: Plenum Press, 1995.

30. Jansen, E. D., and et al., "Temperature dependence of the absorption coefficient of water for mid-infrared laser radiation," *Lasers in Surgery and Medicine*, Vol. 14, pp. 258–268, 1994.

31. Lange, B. L., and T. Brendel, "Temperature dependence of light absorption in water at holmium and thulium laser wavelenghts," *Applied Optics*, Vol. 41, pp. 5797–5803, 2002.

32. Spells, K. E., "The thermal conductivities of some biological fluids," *Physics in Medicine and Biology*, Vol. 5, pp. 139–153, 1960.

33. Cooper, T. E., and G. J. Trezek, "Correlation of thermal properties of some human tissues with water content," *Aerosp Med*, Vol. 42, pp. 24–27, 1971.

34. Tunc, B., and M. Gulsoy, "Tm:fiber laser ablation with real-time temperature monitoring for minimizing collateral thermal damage: ex vivo dosimetry for ovine brain," *Lasers in Surgery and Medicine*, Vol. 45, pp. 48–56, 2013.

35. Bilici, T., and et al., "Development of thulium (tm:yap) laser system for brain tissue ablation," *Lasers in Surgery and Medicine*, Vol. 26, pp. 699–706, 2011.

36. Welch, A. J., and et al., "Laser in thermal ablation," *Photochemistry and Photobiology*, Vol. 53, pp. 815–823, 1991.

37. Tunc, B., and M. Gulsoy, "Temperature measurement during laser brain ablation by thulium fiber laser," *Optical Interactions with Tissue and Cells.*, 2012.